
National University of Singapore

Honours Thesis

# Numerical and Perturbative Studies of Complex Potentials

Author:

Tan Mao Tian

Supervisor:

Dr Wang Qinghai

A thesis submitted to the Physics Department for the fulfilment of the requirements of PC4199, Honours Project in Physics.

April 2014

# Acknowledgement

I would like to express my heartfelt gratitude to my project supervisor, Dr Wang Qinghai, for his guidance and patience, without which this project would not have been possible. Under his guidance and supervision I have learnt a lot about the project and the techniques involved.

## Abstract

We studied the eigenvalues of some complex potentials using two different methods. The first method is perturbation theory, which is an analytical method. The second method is the numerical shooting method. We look at the eigenvalue as a function of a coupling constant. Some of the potentials possess a real spectrum, while for others, complex eigenvalues appear. A pattern for the appearance of complex eigenvalues is observed, in agreement with a related conjecture.

# Contents

# 1. Introduction

One of the axioms of quantum mechanics is the Hermiticity of the Hamiltonian operator. This condition is sufficient to guarantee a real eigenvalue spectrum, but it is not necessary. It is thus natural to ask if there are other possible conditions that can also give rise to real eigenvalues.

In 1993, Bender learnt that two of his colleagues Bessis and Zinn-Justin had studied a non-Hermitian Hamiltonian $H = \hat{p}^2 + i\hat{x}^3$ numerically and noticed that it possessed real eigenvalues [1]. He found out that almost a decade ago, in 1982, Andrianov, had studied $-x^4$ potentials perturbatively. Andrianov's analysis suggested that these potentials might possess a real spectra, despite being non-Hermitian (because the boundary conditions are imposed on the complex $x$-plane) [2]. This led Bender and his student Boettcher to wonder if the spectra of these Hamiltonians were entirely real.

In 1998, Bender and Boettcher published a paper in which they studied a whole family of Hamiltonians [3],

$$H = \hat{p}^2 + \hat{x}^2(i\hat{x})^{\epsilon} \tag{1.1}$$

Here, $\epsilon$ is real. They showed that when $\epsilon \geq 0$, the spectra was entirely real and positive [3]. This family of Hamiltonians include some of the non-Hermitian Hamiltonians that were previously discovered to possess some real eigenvalues. Furthermore, it was observed that this family of Hamiltonians commute with the $\mathcal{PT}$ operator, where, the parity operator $\mathcal{P}$ and the time reversal operator $\mathcal{T}$ have the action

$$\mathcal{P}\hat{x}\mathcal{P} = -\hat{x} \qquad \mathcal{P}\hat{p}\mathcal{P} = -\hat{p} \tag{1.2}$$

$$\mathcal{T}\hat{x}\mathcal{T} = \hat{x} \qquad \mathcal{T}\hat{p}\mathcal{T} = -\hat{p} \tag{1.3}$$

Also, the time-reversal operator performs complex conjugation.

$$\mathcal{T}i\mathcal{T} = -i \tag{1.4}$$

These Hamiltonians are said to be $\mathcal{PT}$-symmetric. This remarkable discovery of an alternative condition to Hermiticity led to a flurry of research into $\mathcal{PT}$ -symmetric non-Hermitian Hamiltonians.

One of the interesting phenomena that occur with such Hamiltonians is known as $\mathcal{PT}$ -symmetry breaking. In short, this occurs when some of the eigenvalues become complex. For the family of Hamiltonians in (1.1), when $-1 < \epsilon < 0$, complex eigenvalues are obtained. This is a rich phenomenon because some Hamiltonians possess this behaviour while others do not, which raises an interesting question on the origin of $\mathcal{PT}$ symmetry breaking.

Even though this area of research originated from considerations of an axiom of quantum mechanics, its major application surprisingly turns out to be in optics. The main link to optics is through the paraxial equation of diffraction,

$$i\frac{\partial E}{\partial z} + \frac{1}{2k}\frac{\partial^2 E}{\partial x^2} + k_0[n_R(x) + in_I(x)]E = 0 \qquad 1.5$$

Notice that if we were to treat the z coordinate as time t, the complex refractive index $n_R(x) + in_I(x)$ as a potential, the electric field as a wave function, after relabeling some of the constants, we end up with the Schrödinger equation! It turns out that it is possible to implement a $\mathcal{PT}$ -symmetric optical system, and some of these systems also experience $\mathcal{PT}$ symmetry breaking. Thus, $\mathcal{PT}$ symmetry breaking is an important phenomenon to study.

On the cause of $\mathcal{PT}$ symmetry breaking, Bender conjectured that for two-dimensional quantum mechanical systems, $\mathcal{PT}$ symmetry breaking occurs whenever a Hermitian term is combined with a non-Hermitian $\mathcal{PT}$ symmetric one [12].

In this project, several examples of one-dimensional complex potentials were studied to search for $\mathcal{PT}$ symmetry breaking. An example of a Hamiltonian with broken $\mathcal{PT}$ symmetry is

$$H = \hat{p}^2 + \hat{x}^2 - igx^5 \qquad 1.6$$

The potential is a combination of a Hermitian term $\hat{x}^2$ and a non-Hermitian $\mathcal{PT}$ symmetric term $-igx^5$. We find that the results of this project are in agreement with Bender's conjecture even though we are studying one-dimensional potentials and we see that the behaviour of complex potentials is rich and complex.

# 2. $\mathcal{PT}$ symmetry

## 2.1 $\mathcal{PT}$ -symmetric non-Hermitian quantum mechanics

In 1998, Bender and Boettcher wrote a paper that discussed the real spectra of $\mathcal{PT}$ -symmetric non-Hermitian Hamiltonians [3]. Many important results are summarised in [1]. We mention briefly the important details, before mentioning a link between $\mathcal{PT}$ symmetric quantum mechanics and optics, which is the main application of the theory.

## 2.2 Parity and Time operators

There are two more important properties for the $\mathcal{P}$ and $\mathcal{T}$ operators defined in (1.2), (1.3) and (1.4).

They are reflection operators, so we have

$$\mathcal{P}^2 = \mathcal{T}^2 = 1 \qquad 2.1$$

The last important property about them is that they commute.

$$\mathcal{PT} - \mathcal{TP} = 0 \qquad 2.2$$

## 2.3 A general class of $\mathcal{PT}$ -symmetric Hamiltonians

Let us return to the Hamiltonians in (1.1). The spectra of the Hamiltonians have very different behaviours for different ranges of the parameter $\epsilon$. When this parameter is 0, the Hamiltonian is the usual harmonic oscillator Hamiltonian. As this parameter increases from 0, the Hamiltonian becomes non-Hermitian. The following figure is obtained from [1].

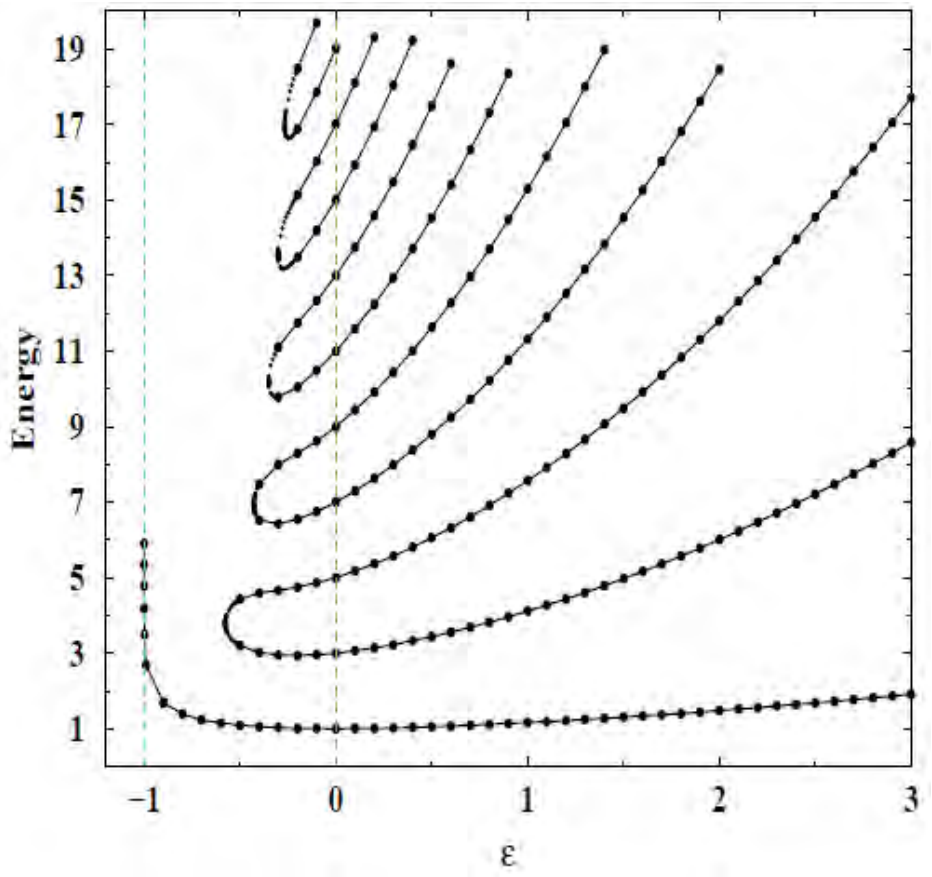


Fig 1 : Eigenvalues for Hamiltonian in (1.6) for varying values of ε. Taken from [1]

When $\epsilon \geq 0$, all the eigenvalues are real and positive and the energy levels rise with increasing ε. As ε drops from 0 to -1, the number of real eigenvalues decrease, until $\epsilon = -0.57793$, then there is only the ground state eigenvalues left. Some of the Hamiltonians we shall study in this project are similar to the (1.1), except that we have an extra $\hat{x}^2$term so that the unperturbed Hamiltonian, the portion without the complex term, is the usual Harmonic oscillator. Later on, we shall change the $\hat{x}^2$ term to other terms to look at the effects on the eigenvalue spectrum.

## 2.4 Important properties of a quantum theory

There are three properties the $\mathcal{PT}$ -symmetric quantum mechanics must fulfil.

i. The Hamiltonian determines the energy levels of a quantum theory. The energy levels are the eigenvalues in the following equation.

$$H\psi = E\psi \qquad 2.3$$

ii. The Hamiltonian determines the time evolution of the states and operators in the quantum theory. Time evolution is governed by

$$H\psi = i\frac{\partial \psi}{\partial t} \tag{2.4}$$

Assuming H is independent of time, we obtain the solution as

$$\psi(t) = e^{-iHt}\psi(0) \tag{2.5}$$

We require $e^{-iHt}$ to be unitary so that the norm of the state will always be unity.

iii. The Hamiltonian incorporates the symmetries of the theory. If a Hamiltonian H commutes with $\mathcal{P}$, and since $\mathcal{P}$ is a linear operator, $\mathcal{P}$ and H will share their eigenstates. So any eigenstate of a Hamiltonian that is parity invariant will have a definite parity (even or odd under space inversion).

## 2.5 Broken and Unbroken $\mathcal{PT}$ Symmetry

A $\mathcal{PT}$ symmetric Hamiltonian commutes with the $\mathcal{PT}$ operator. Since the $\mathcal{PT}$ operator is antilinear, we cannot conclude that the eigenstates of H will be eigenstates of $\mathcal{PT}$. However, suppose that an eigenstate of H, $\psi$, is also an eigenstate of $\mathcal{PT}$. Then, calling its eigenvalue $\lambda$, we get the following

$$PT\psi = \lambda\psi \tag{2.6}$$

Multiply $\mathcal{PT}$ on the left and use the fact that $(PT)^2 = 1$, and we obtain

$$\psi = PT\lambda(PT)^2\psi \tag{2.7}$$

Since $\mathcal{PT}$ is antilinear, we get

$$\psi = \lambda^*\lambda\psi = |\lambda|^2\psi \tag{2.8}$$

This implies that $|\lambda|^2 = 1$, so $\lambda$ is a pure phase

$$\lambda = e^{i\alpha} \tag{2.9}$$

Multiplying the time independent Schrödinger equation by $\mathcal{PT}$, we obtain

$$(PT)H\psi = PTE(PT)^2\psi \quad 2.10$$

$$H\lambda\psi = (PT)E(PT)\lambda\psi \quad 2.11$$

$$E\lambda\psi = E^*\lambda\psi \quad 2.12$$

Since $\lambda \neq 0$, we conclude that $E = E^*$, i.e. the eigenvalue E is real. Thus, an eigenstate of H that is also an eigenstate of $\mathcal{PT}$ will have a real eigenvalue. So, we make the following definition: If every eigenfunction of a $\mathcal{PT}$ symmetric Hamiltonian is also an eigenfunction of the $\mathcal{PT}$ operator, we say that the $\mathcal{PT}$ symmetry of H is unbroken. If some of the eigenfunctions of a $\mathcal{PT}$ symmetric Hamiltonian are not simultaneously eigenfunctions of the $\mathcal{PT}$ operator, we say that the $\mathcal{PT}$ symmetry of H is broken.

With the result we just showed, we can conclude that all the eigenvalues of a $\mathcal{PT}$ symmetric Hamiltonian with unbroken $\mathcal{PT}$ symmetry will have all real eigenvalues. If some eigenvalues are complex, then $\mathcal{PT}$ symmetry is broken.

In this report, we will see that for certain ranges of a coupling constant, we will have all real eigenvalues, while for other values of the coupling constant, we will obtain some complex eigenvalues, and the $\mathcal{PT}$ symmetry is broken. $\mathcal{PT}$ symmetry breaking is worth studying because this phenomenon also occurs in optics, as we will discuss in the following section.

## 2.6 $\mathcal{PT}$ symmetry and optics

In [4], an observation of the behaviour of a $\mathcal{PT}$ symmetric optical coupled system is reported. Spontaneous $\mathcal{PT}$ symmetry breaking is also observed. As mentioned in the introduction, the key to linking optics to $\mathcal{PT}$ symmetric quantum mechanics is to look at the paraxial equation of diffraction (1.5). In (1.5), $k_0 = \frac{2\pi}{\lambda}$, $k = k_0 n_0$, $\lambda$ is the wavelength of light in vacuum and $n_0$ represents the substrate index. More importantly, the complex refractive-index distribution $n(x) = n_R(x) + in_I(x)$ plays the role of an optical potential. In order for this "potential" to be $\mathcal{PT}$ symmetric, we require the refractive index profile $n_R$ be even, while gain/loss distribution $n_I$ be odd. If we treat the coordinate z to be time, the electric field E to be the wave function, and identify the constants accordingly, we notice that

equation (1.5) is equivalent to the time dependent Schrödinger equation. We can then proceed to separate variables and obtain the time independent "Schrödinger equation".

In [5], a $\mathcal{PT}$ symmetric ridge optical waveguide demonstrates $\mathcal{PT}$ symmetry breaking. It is more interesting to note that once the gain/loss contrast exceeds $\alpha_c \cong 50\ cm^{-1}$, the set of eigenvalues become partly complex. In a certain optical system, the eigenvectors before the critical point are given by $(1, \pm e^{\mp i\theta})$ with eigenvalues $\mp \cos\theta$, where $\theta$ is some parameter. Above the critical point, the eigenvectors become $(1, -ie^{\mp\theta})$ with eigenvalues $\mp i \sinh\theta$. The key thing to note is that the critical point here behaves in a similar fashion to the critical point $\epsilon = -0.57793$ in figure 1. Below the critical point, the eigenvalues are real, while above it, complex eigenvalues are obtained.

Another interesting paper in which the connection between $\mathcal{PT}$ symmetric quantum mechanics and optics is explored is [11]. In this paper, a system of a one-dimensional array with N identical, single-mode waveguides is explored. For a certain system with N = 2, the Hamiltonian is

$$H = \frac{h}{2\pi}\begin{bmatrix} i\gamma & -C \\ -C & -i\gamma \end{bmatrix} \qquad 2.13$$

where C is the tunnelling amplitude between the two waveguides. This Hamiltonian is clearly non-Hermitian, but it is $\mathcal{PT}$ symmetric because applying parity reflection (*P*: waveguide 1 ↔ waveguide 2) and time reversal ($T: i \rightarrow -i$) does not change the matrix.

## 2.7 The Harmonic oscillator with a complex quintic perturbation

In 2008, Smilga published a paper [7] that had a numerical study of the Hamiltonian

$$H = \frac{\hat{p}^2 + \hat{x}^2}{2} - igx^5 \qquad 2.14$$

The perturbation series for the ground state energy is given by

$$E_0 = \frac{1}{2} + \frac{449g^2}{32} + O(g^4) \qquad 2.15$$

He plots the eigenvalues obtained numerically for the ground state:

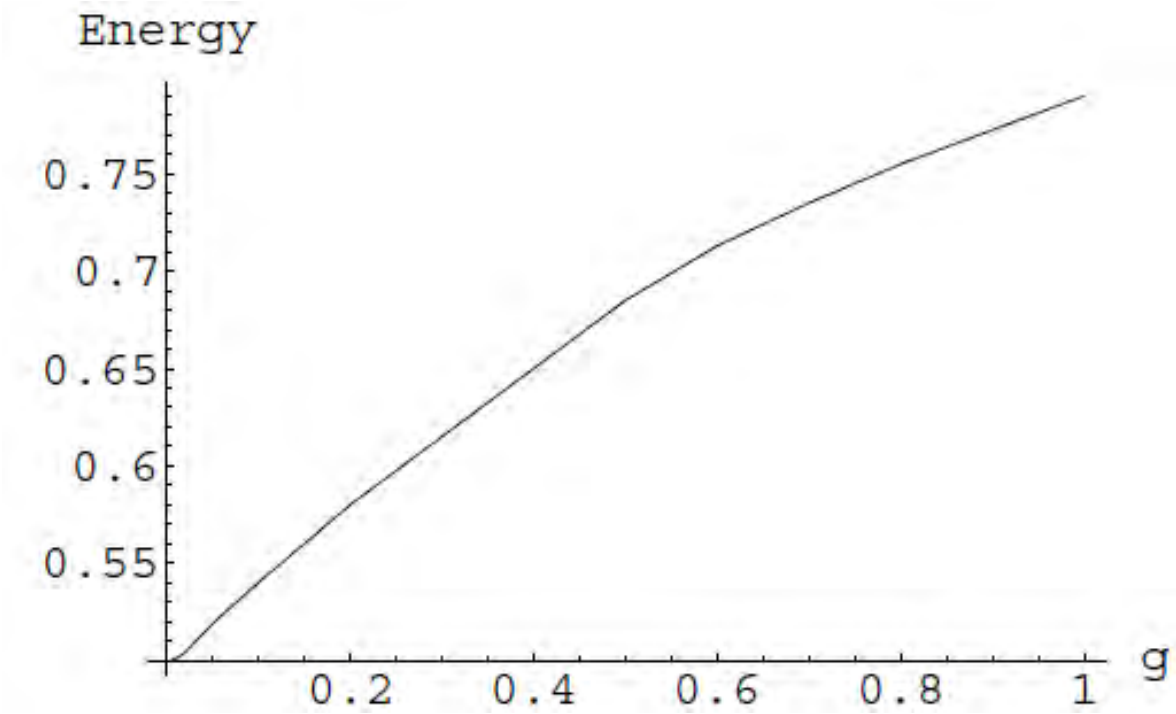


Fig 2: Eigenvalues for the ground state of the Hamiltonian (2.19) as shown in [7]

He then looks at another eigenvalue problem. This time, the wave function $\psi(x)$ is analytically continued into the complex plane (i.e. x becomes a complex variable). This approach is described in [8]. The relevant details will be described later on in the relevant sections. For this eigenvalue problem, the variable x lie on the rays with arguments $-\frac{3\pi}{14}$ and $\frac{17\pi}{14}$ respectively. Here, an interesting phenomenon occurs when g goes to zero. It is observed that the ground state and the first excited state get closer until they merge at a critical value of $g = 0.3717$ and their energies coincide. The energy of the second excited state decreases with decreasing g and approaches the energy of the ground state. Below is the logarithmic plot which demonstrates this behaviour.

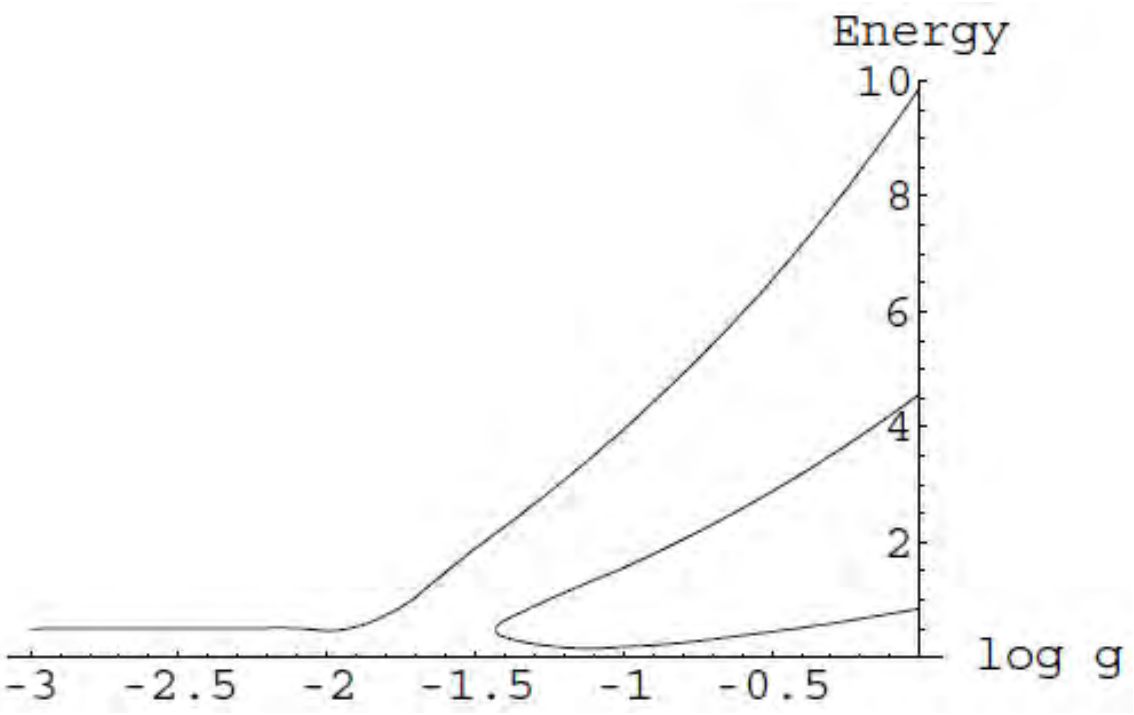


Fig 3: Logarithmic plot of the eigenvalues of (2.19) as shown in [7]

## 2.8 Two dimensional $\mathcal{PT}$ symmetric potentials

In 2009, Wang [10] published a paper that shows the eigenvalues for some examples of two dimensional $\mathcal{PT}$ symmetric potentials. The first example was a complex cubic potential

$$H_{12} = p_x^2 + p_y^2 + x^2 + y^2 + igxy^2 \qquad 2.16$$

Plots of the real and imaginary parts of the eigenvalues are shown on the next page. From figure 5, we can see that the eigenvalues come in complex conjugate pairs. It can be seen from (2.11) that if E is an eigenvalue, then $E^*$ is also an eigenvalue.

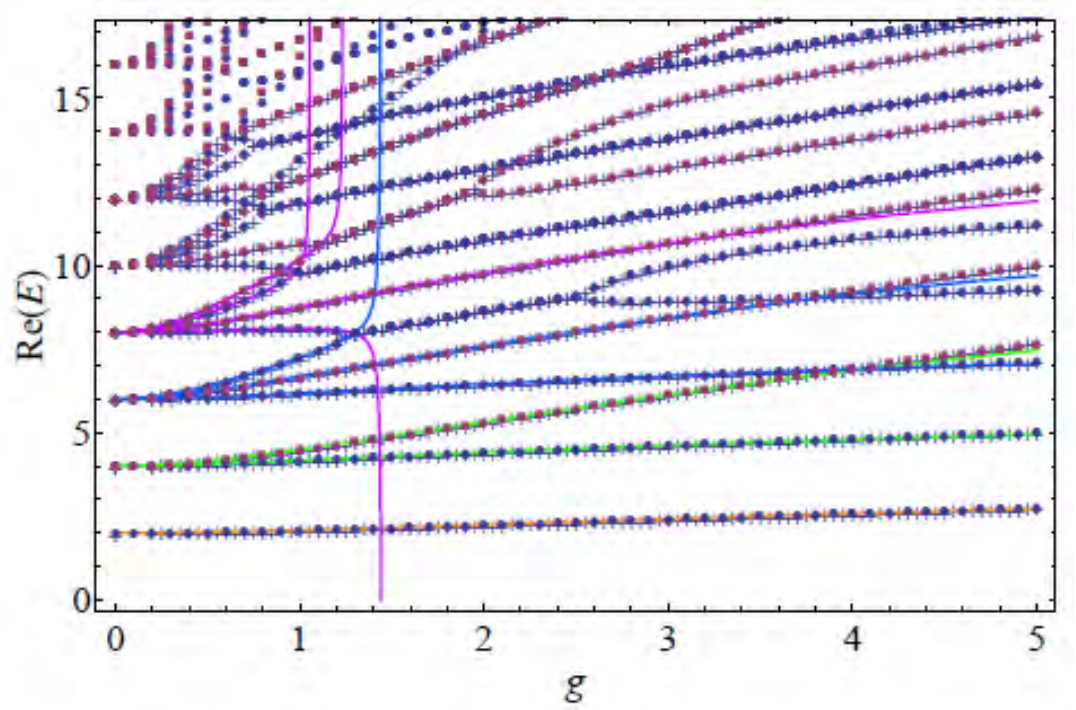


Fig 4: Real parts of the eigenvalues as functions of the coupling constant g with the complex cubic potential. Lines are from perturbative expansion using (20,20) Padé. Crosses are the results using FEM. Dots are results using the method based on two-dimensional HO basis expansions. The system is symmetric under g → -g and only the part with positive g is shown. Taken from [10].

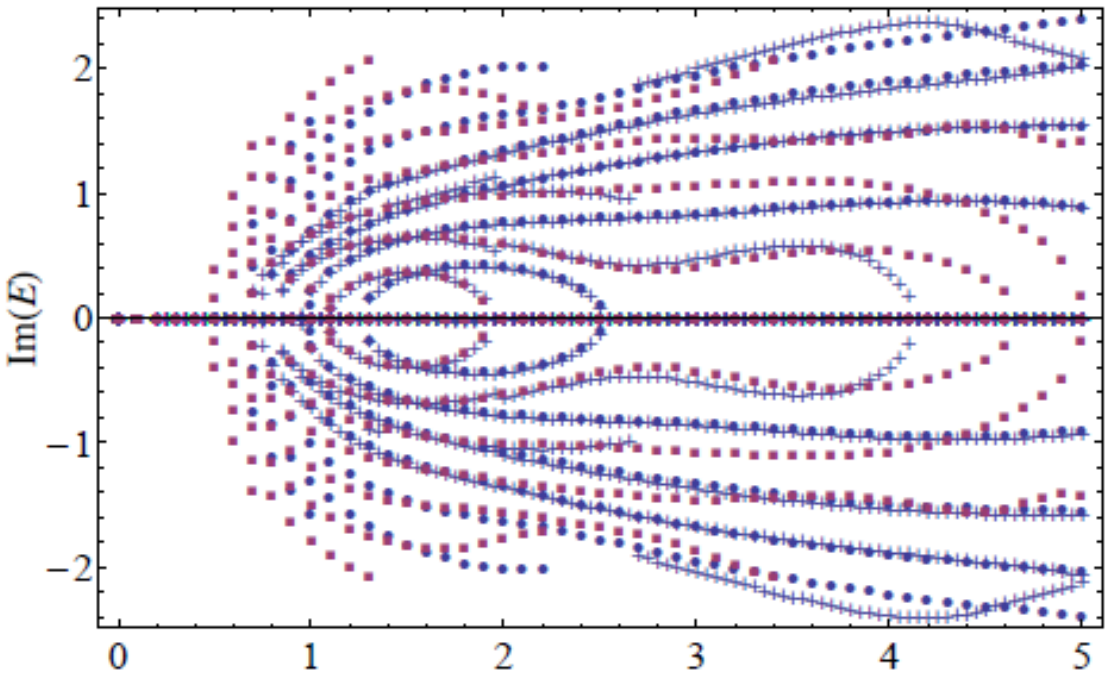


Fig 5: Imaginary parts of the eigenvalues as functions of the coupling constant g with the complex cubic potential. Crosses are the results using FEM. Dots are the results using the method based on two-dimensional HO basis expansions. The system is symmetric under g → -g, only the part with the positive g is shown. Taken from [10].

The second Hamiltonian studied in the paper is the complex Hénon-Heiles Hamiltonian

$$H_{HH} = p_x^2 + p_y^2 + x^2 + y^2 + ig\left(xy^2 - \frac{1}{3}x^3\right) \tag{2.17}$$

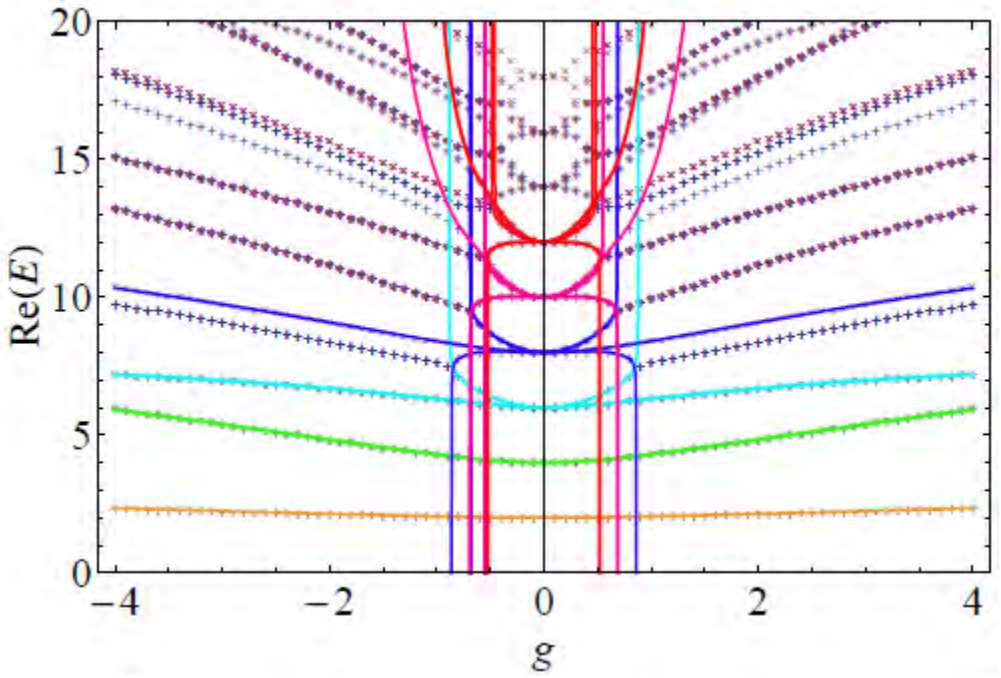


Fig 6: Real parts of the eigenvalues as functions of the coupling constant g with the complex Hénon-Heiles potential. Lines are from perturbative expansion using (20,20) Padé. Crosses are from HO basis expansions. Taken from [10].

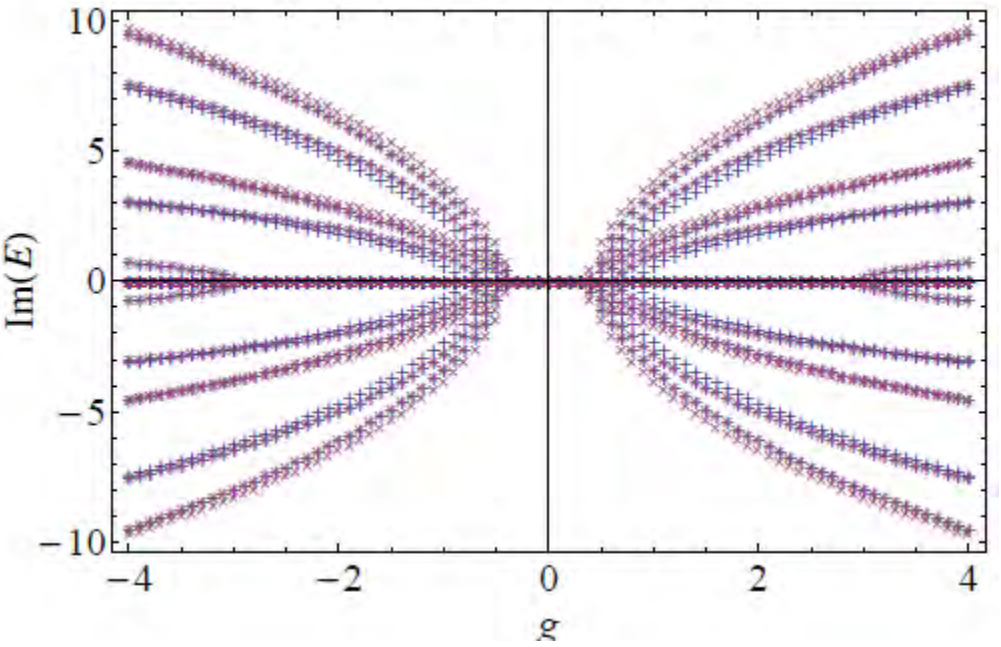


Fig 7: Imaginary parts of the eigenvalues as functions of the coupling constant g with the complex Hénon-Heiles potential. Only eigenvalues from HO basis expansions are shown. Taken from [10].

# 3. The quartic perturbation

The first Hamiltonian we studied is the harmonic oscillator with the quartic perturbation is shown below.

$$H = \hat{p}^2 + \hat{x}^2 + g\hat{x}^4 \tag{3.1}$$

We will follow the procedure outlined in Bender's paper on the anharmonic oscillator [6]. We are working in units where the factors in front of $p^2$ and $x^2$ are equal to unity. This helps to make the calculation less messy.

## 3.1 Perturbation Theory

The first method we use is Perturbation theory. We start off with the Schrödinger equation.

$$\left(-\frac{d^2}{dx^2} + x^2 + gx^4\right)\psi(x) = E\psi(x) \tag{3.2}$$

Let

$$\psi(x) = e^{-\frac{x^2}{2}}\phi(x) \tag{3.3}$$

Then

$$\psi''(x) = e^{-\frac{x^2}{2}}[\phi''(x) - 2x\phi'(x) + (x^2 - 1)\phi(x)] \tag{3.4}$$

Substituting (3.3) and (3.4) into (3.2), we get

$$-\phi''(x) + 2x\phi'(x) + (1 + gx^4)\phi(x) = E\phi(x) \tag{3.5}$$

Then we expand the energy and ϕ(x) as power series of g, the perturbation parameter.

$$E = \sum_{r=0}^{\infty} g^r A_r \tag{3.6}$$

$$\phi(x) = \sum_{r=0}^{\infty} g^r B_r(x) \tag{3.7}$$

Here, we have fixed n, and have left out the subscript for convenience. In the usual perturbation series, we expand the wave function in terms of the unperturbed wave function for the Harmonic oscillator. However, we have substituted $B_r(x)$, which will be a

polynomial in x, since the exponential term has been factored out and all that remains are linear combinations of Hermite Polynomials.

Note that

$$A_0 = 2n + 1 \tag{3.8}$$

While $B_0 e^{-\frac{x^2}{2}}$ is the unperturbed wave function of the harmonic oscillator.

Substituting (3.6) and (3.7) into (3.5) yields

$$-\sum_{r=0}^{\infty} g^r B_r''(x) + 2x \sum_{r=0}^{\infty} g^r B_r'(x) + (1 + gx^4) \sum_{r=0}^{\infty} g^r B_r(x) = \sum_{r=0}^{\infty} \sum_{s=0}^{\infty} g^{r+s} A_r B_s(x) \tag{3.9}$$

Let $r' = r + s$. Since $r \geq 0,\ r' \geq s$, so

$$-\sum_{r=0}^{\infty} g^r B_r''(x) + 2x \sum_{r=0}^{\infty} g^r B_r'(x) + (1 + gx^4) \sum_{r=0}^{\infty} g^r B_r(x) = \sum_{r\prime=0}^{\infty} \sum_{s=0}^{r\prime} g^{r\prime} A_{r'-s} B_s(x) \tag{3.10}$$

Since r' is just a dummy variable, we can replace it with r, to get

$$\sum_{r=0}^{\infty} g^r \left(-B_r''(x) + 2xB_r'(x) + B_r(x)\right) + \sum_{r=1}^{\infty} g^r x^4 B_{r-1}(x) = \sum_{r=0}^{\infty} \sum_{s=0}^{r} g^r A_{r-s} B_s(x) \tag{3.11}$$

Each power of $g^r$ yields an equation. For $r = 0$, we get

$$-B_0''(x) + 2xB_0'(x) + B_0(x) = A_0 B_0(x) \tag{3.12}$$

For $r \geq 1$, we get equations for the unknowns $A_r$ and $B_r$. Let us solve this for the ground state. Then, $A_0 = 1$, and since we factored out the exponential from the wave function in (3.3), $B_0$ is just the Hermite polynomial for the ground state, so $B_0 = 1$. (3.11) then becomes

$$-B_r''(x) + 2xB_r'(x) + x^4 B_{r-1}(x) = A_r B_0(x) + \sum_{s=1}^{r-1} A_{r-s} B_s(x) \tag{3.13}$$

Where the sum on the right hand side vanishes for r=1.

Now, we substitute an ansatz for$B_r(x)$, where $r \geq 1$.

$$B_r(x) = \sum_{j=1}^{2r} x^{2j} B_{r,j} \qquad 3.14$$

This step is different from the usual substitution we do for perturbation theory. In undergraduate quantum mechanics textbooks like [8], the perturbed wave function is usually expressed as a linear combination of the unperturbed wave functions since those states form a complete orthonormal set. Since those unperturbed wave functions are just linear combinations of Hermite polynomials with an exponential factor, we can just express the $r^{th}$ correction to the wave function as a polynomial after pulling out the exponential factor. The advantage of working with these simple polynomials is that they are much easier to evaluate.

The coefficient of $g^r$ in the usual perturbation series, is given by

$$(H_0 - E^{(0)})\psi^{(r)} = \sum_{s=1}^{r} E^{(s)}\psi^{(r-s)} - H'\psi^{(r-1)} \qquad 3.15$$

Where $H_0$is the unperturbed harmonic oscillator Hamiltonian, H' is the perturbation, $E^{(r)}$ is the r$^{th}$ order correction to the energy and $\psi^{(r)}$ is the r$^{th}$ order correction to the wave function. Consider the first order correction to the ground state (i.e. r =1 ).

$$(H_0 - E^{(0)})\psi^{(1)} = (E^{(1)} - H')\psi^{(0)} = (E^{(1)} - \hat{x}^4)\psi^{(0)} \qquad 3.16$$

Since $\hat{x}$ contains both the raising and lowering operators $\hat{a}^+$ and $\hat{a}$, the right hand side would contain terms of up to $|4>$. So, for the first correction, we would have polynomials of degree 4. We can repeat this argument inductively to show that the r$^{th}$ term is a polynomial of degree 4r.

Note that in the expansion (3.14), the constant term is missing. This is because in the usual perturbation theory where we expand the perturbed wave functions as a linear combination of the unperturbed wave functions, the coefficient of $g^r$ gives (3.15). The terms on the right hand side are known, assuming that we have calculated until the (r-1)$^{th}$ correction. Then we have a linear inhomogeneous equation for $\psi^{(r)}$. Adding a solution to the homogeneous equation to a solution to the inhomogeneous equation will give another solution to the inhomogeneous equation, so we have the freedom to subtract the homogeneous solution,

in this case the unperturbed ground state wave function, from $\psi^{(r)}$. This is why there are no constant terms in (3.14), because we have the freedom to subtract away the constant terms since the Hermite polynomial for the ground state is a constant term.

We have also only used even terms in the expansion (3.14) because for the ground state, the wave function is even. We know that the unperturbed ground state is even, and looking at (3.16), if we replaced x with –x, we would get back the same equation except that the argument of $\psi^{(1)}$ would be –x. This is because the $H_0$and $H'$ terms are even as well, and this tells us that $\psi^{(1)}$ is even. We can continue this inductively to show that for all non-negative integers r, $\psi^{(r)}$ is even.

Then the second derivative is given by

$$B_r''(x) = \sum_{j=1}^{2r} 2j(2j-1)x^{2j-2}B_{r,j} \tag{3.17}$$

Now, we substitute 3.14 and 3.17 into 3.13

$$\begin{aligned} -\sum_{j=0}^{2r-1}(2j+2)(2j+1)x^{2j}B_{r,j+1} + \sum_{j=1}^{2r}4jx^{2j}B_{r,j} + \sum_{j=3}^{2r+2}x^{2j}B_{r-1,j-2} \\ = A_r + \sum_{j=1}^{2r}x^{2j}\sum_{s=1}^{r-1}A_{r-s}B_{s,j} \end{aligned} \tag{3.18}$$

Each coefficient of $x^{2j}$ yields an equation.

$$x^0: \quad -2B_{r,1} = A_r \tag{3.19}$$

$$x^2, x^4: \quad -(2j+2)(2j+1)B_{r,j+1} + 4jB_{r,j} = -2\sum_{s=1}^{r-1}B_{r-s,1}B_{s,j} \tag{3.20}$$

$$\begin{gathered} x^{2j}, j = 3, \dots, 2r-1: \\ -(2j+2)(2j+1)B_{r,j+1} + 4jB_{r,j} + B_{r-1,j-2} = -2\sum_{s=1}^{r-1}B_{r-s,1}B_{s,j} \end{gathered} \tag{3.21}$$

$$x^{4r}\ (or\ j = 2r): \qquad 8rB_{r,2r} + B_{r-1,j-2} = -2\sum_{s=1}^{r-1}B_{r-s,1}B_{s,2r} \tag{3.22}$$

These recursion relations hold for $r \geq 2$. For the case where $r = 1$, apply (3.13) and (3.14) directly.

With the recursion relations, we can solve for the energy eigenvalues. Starting from (3.22), we can solve for $B_{r,j}$ for $j = 1,2,\dots,2r$, and then we can use (3.19) to find the energy eigenvalue. Using Mathematica to compute the coefficients, we get

$$E_0 = 1 + \frac{3}{4}g - \frac{21}{16}g^2 + \frac{333}{64}g^3 - \frac{30885}{1024}g^4 + \frac{916731}{4096}g^5 - \frac{65518401}{32768}g^6 + \cdots \quad 3.23$$

This is the perturbation series for the ground state. We calculate up to the 200$^{th}$ order correction.

Next, we move on to the first excited state. This time, we make the substitution

$$B_r = \sum_{j=1}^{2r} x^{2j+1} B_{r,j} \quad 3.24$$

We use odd terms instead because the 1$^{st}$ excited state has a wave function that is odd. As before, we do not use the x term because we have the freedom to subtract of a multiple of the unperturbed solution, which is a multiple of x.

Proceeding in the same manner, we obtain the recursion relations for $r \geq 2$.

$$B_{r,2r} = \frac{1}{8r}\left[-B_{r-1,2r-2} - 3\sum_{s=1}^{r-1} B_{r-s,1}B_{s,2r}\right] \quad 3.25$$

$$j = 3,\dots,2r-1:$$

$$B_{r,j} = \frac{1}{4j}\left[(2j+2)(2j+3)B_{r,j+1} - B_{r-1,j-2} - 3\sum_{s=1}^{r-1} B_{r-s,1}B_{s,j}\right] \quad 3.26$$

$$j = 1,2: \qquad B_{r,j} = \frac{1}{4j}\left[(2j+2)(2j+3)B_{r,j+1} - 3\sum_{s=1}^{r-1} B_{r-s,1}B_{s,j}\right] \quad 3.27$$

$$A_r = -3B_{r,1} \quad 3.28$$

For $r = 1$, use (3.13) directly.

Using Mathematica, the perturbation series is

$$E_1 = 3 + \frac{15}{4}g - \frac{165}{16}g^2 + \frac{3915}{64}g^3 - \frac{520485}{1024}g^4 + \frac{21304485}{4096}g^5 - \frac{2026946145}{32768}g^6 + \cdots \quad 3.29$$

For the 2nd excited state, we use the freedom to subtract multiples of the unperturbed state to remove the $x^2$ term, so we substitute

$$B_r = \sum_{j=1}^{2r} x^{2j+2} B_{r,j} + B_{r,0} \quad 3.30$$

The recursion relations are as follows

$$B_{r,2r} = \frac{1}{8r}[-B_{r-1,2r-2} - 3\sum_{s=1}^{r-1} B_{r-s,1}B_{s,2r}] \quad 3.31$$

$$j = 3, \ldots, 2r-1:$$

$$B_{r,j} = \frac{1}{4j}[(2j+3)(2j+4)B_{r,j+1} - B_{r-1,j-2} - 3\sum_{s=1}^{r-1} B_{r-s,1}B_{s,j}] \quad 3.32$$

$$B_{r,2} = \frac{1}{8}[56B_{r,3} - 3\sum_{s=1}^{r-1} B_{r-s,1}B_{s,2}] \quad 3.33$$

$$B_{r,1} = \frac{1}{4}[30B_{r,2} - B_{r-1,0} - 3\sum_{s=1}^{r-1} B_{r-s,1}B_{s,1}] \quad 3.34$$

$$A_r = -3B_{r,1} \quad 3.35$$

We calculate the perturbation series to be

$$E_2 = 5 + \frac{39}{4}g - \frac{615}{16}g^2 + \frac{20079}{64}g^3 - \frac{3576255}{1024}g^4 + \frac{191998593}{4096}g^5 - \frac{23513776995}{32768}g^6 + \cdots \quad 3.36$$

We can continue in this manner to calculate the perturbation series for higher energy levels. Letting $E_n$ be the perturbation series for the nth excited state, we get

$$E_3 = 7 + \frac{75}{4}g - \frac{1575}{16}g^2 + \frac{66825}{64}g^3 - \frac{15184575}{1024}g^4 + \frac{1024977375}{4096}g^5 - \frac{155898295875}{32768}g^6 + \cdots \quad (3.37)$$

$$E_4 = 9 + \frac{123}{4}g - \frac{3249}{16}g^2 + \frac{171153}{64}g^3 - \frac{47745225}{1024}g^4 + \frac{3918561111}{4096}g^5 - \frac{718596848709}{32768}g^6 + \cdots \quad (3.38)$$

$$E_5 = 11 + \frac{183}{4}g - \frac{5841}{16}g^2 + \frac{369063}{64}g^3 - \frac{122636745}{1024}g^4 + \frac{11913835401}{4096}g^5 - \frac{2571309540261}{32768}g^6 + \cdots \quad (3.39)$$

The perturbation series are calculated to the 200th correction. We then convert this into a Padé approximant. A Padé approximant is a rational approximation to a function. As an example, suppose we have only found the ground state perturbation series up to the fourth order correction.

$$E_0 = 1 + \frac{3}{4}g - \frac{21}{16}g^2 + \frac{333}{64}g^3 - \frac{30885}{1024}g^4 \quad (3.40)$$

There are five undetermined coefficients, so we can approximate it with a rational function with a degree 2 polynomial in the numerator and in the denominator.

$$\frac{\sum_{i=0}^{2} A_i g^i}{\sum_{j=0}^{2} B_j g^j} \quad (3.41)$$

It might seem like there are 6 undetermined coefficients in this rational functions, but we can divide both the numerator and denominator by $B_0$ to end up with only five unknowns. Then, we can match the Taylor series of (3.41) about $g = 0$ with (3.40) to determine the values of the other undetermined coefficients. We then end up with the following.

$$E_0 \approx \frac{1 + \frac{7931}{992}g + \frac{19567}{1984}g^2}{1 + \frac{7187}{992}g + \frac{22781}{3968}g^2} \quad (3.42)$$

Note that when $g = 0$, we recover the ground state of $E = 1$. This is called a (2,2) Padé approximant, because both the numerator and the denominator have degree 2. If we had a degree 3 polynomial in the numerator and a degree 1 polynomial in the denominator, then it would be called a (3,1) Padé approximant.

We managed to calculate up to the 200th order correction for the energy level, so we solved for a (100,100) Padé approximant. The purpose of calculating the Padé approximant is that the Padé approximant usually gives a better approximation then the truncated power series and has a larger radius of convergence as compared to the perturbation series. The reason is because the original perturbation series is a 200th degree polynomial and so it will "blow-up very quickly" as we increase g. For the (100,100) Padé approximation, for $g > 1$, the numerator and the denominator are dominated by the $x^{100}$ term, and since they are of equal order, the Padé approximant does not "blow up" as quickly as the original perturbation series.

We also calculate the (101,99) and (99,101) Padé approximants. To determine the values of g for which the (100,100) Padé approximant is a good approximation to the eigenvalue, we compare the graphs of the (100,100), (101,99) and (99,101) Padé approximants and look at the region where they agree. This should roughly correspond to the region where the Padé approximant is accurate. The graphs are shown below.

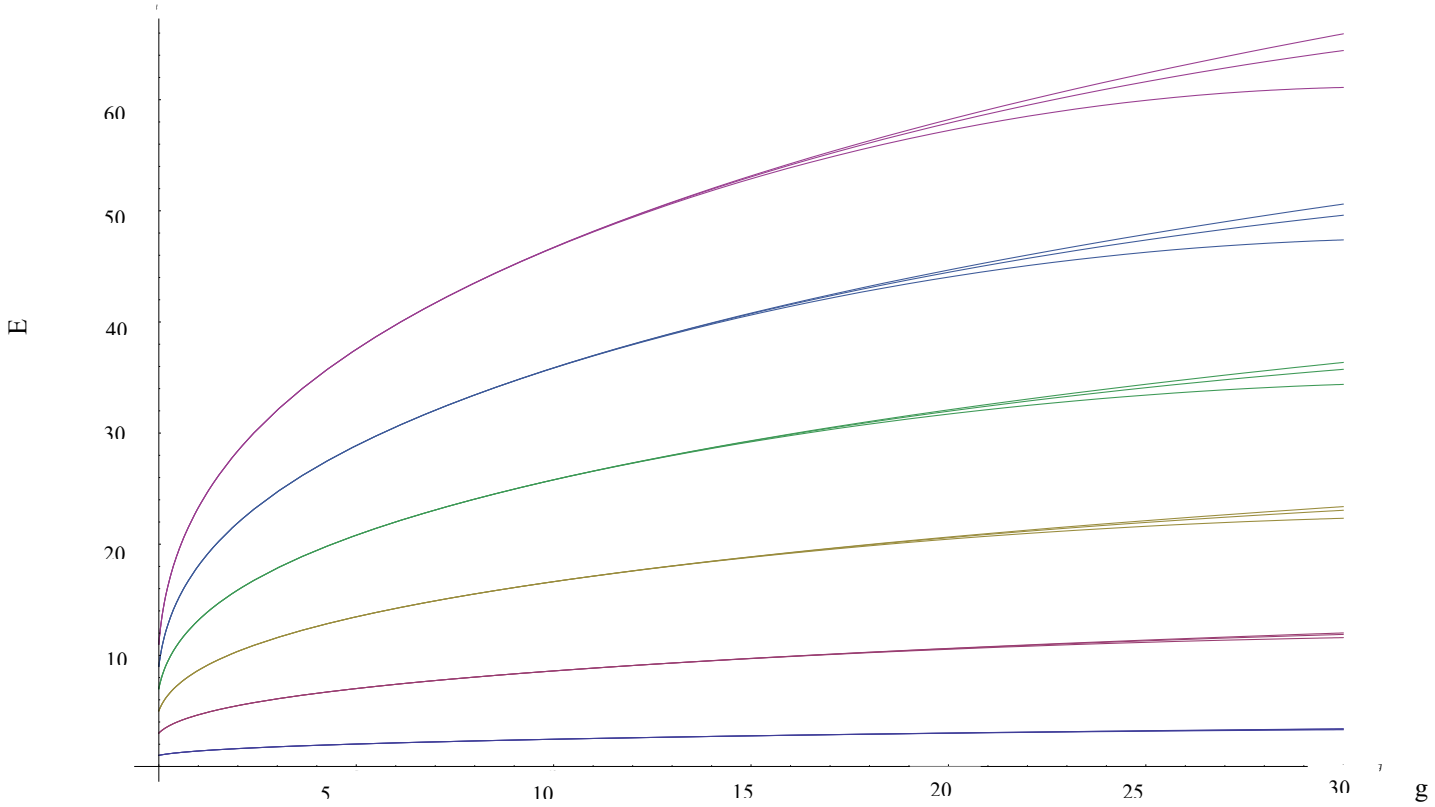


Fig 8: Padé approximant for the eigenvalues perturbation series of $x^2 + gx^4$ potential for g=0 to g=30. For each energy level, the highest most graph corresponds to (100,100) Padé, the second highest corresponds to (101,99) and the lowest graph corresponds to (99,101)

Note that for each energy level, we have plotted the three Padé approximants of order (100,100), (101,99) and (99,101), and for each energy level, the highest graph corresponds to (100,100), the second highest corresponds to (101,99) and the third highest corresponds to (99,101). We consider the Padé to be a good approximation in the regions where the three graphs match up. A table of estimates of the maximum value of g for which the Padé approximants are valid is shown below.

| n | g |
|---|---|
| 0 | ≈30 |
| 1 | 24±2 |
| 2 | 20±2 |
| 3 | 17±2 |
| 4 | 15±2 |
| 5 | 13±3 |

Table 1: Maximum values of g for which the three Padé approximants agree

## 3.2 Shooting method

The next method we use to study the Hamiltonian in (3.1) is a numerical method, namely the shooting method. To do this, we must first determine the boundary condition of the wave functions at "infinity". For the wave functions to be square-integrable, we require the wave function to vanish as x goes to infinity. For our numerical method, we do not have to normalise the wave function because we are simply determining the eigenvalue e, and since (3.2) is linear, any scalar multiple of its solution is still a solution. Normalisation is only required when we wish to find the probability of finding the particle in a certain region. Thus, for convenience, we set

$$\psi(\pm 10) = 1 \tag{3.43}$$

We have used the value $x = \pm 10$ as infinity. If this boundary is too small, then some eigenvalues will not be detected because the boundary must be at "infinity". If the boundary is too large, the integration will take too long and also accumulate a lot of numerical errors for each iteration. To determine $\psi'(\pm 10)$, we shall use the WKB methods. Note that the potential is growing for large x, so for large x we will be in the tunnelling region. So, we use the following formulas obtained from [8]

$$\psi(x) \cong \frac{C}{\sqrt{|p(x)|}} Exp\left[\pm \int |p(x)| dx\right] \qquad , x \to \mp\infty \tag{3.44}$$

Where the absolute value of the momentum is given by

$$|p(x)| = \sqrt{x^2 + gx^4 - E} \tag{3.45}$$

Then, we can differentiate (3.44) to get an expression for $\psi'(x)$ and divide this by (3.44) to eliminate the undetermined constant C and obtain a ratio of $\psi'$ to $\psi$. This ratio is

$$\frac{\psi'(x)}{\psi(x)} = -\frac{x + 2gx^3}{2(x^2 + gx^4 - E)} + \sqrt{x^2 + gx^4 - E} \quad , x \to \infty \tag{3.46}$$

Since we have fixed $\psi(\pm 10) = 1$, by (3.43),

$$\psi'(-10) = -\frac{x + 2gx^3}{2(x^2 + gx^4 - E)} + \sqrt{x^2 + gx^4 - E}, \;\; x = -10 \tag{3.47}$$

We can also impose one more boundary condition to simplify our calculations. As mentioned earlier, the odd states have wave functions that are odd while the even states have wave functions that are even. These requirements can only be satisfied if the following hold.

$$\psi_{odd}(0) = 0 \tag{3.48}$$

$$\psi_{even}{}'(0) = 0 \tag{3.49}$$

So we basically require either the wave function to vanish at the origin (as in the case of odd states) or the first derivative to vanish at the origin (for the even states). So, we use the NDsolve function in Mathematica to integrate (3.2) along the real axis from $x = -10$ to $x = 0$ with the boundary conditions (3.47) and (3.48)/(3.49). We first do the integration for $g = 0$. Since this is just the unperturbed harmonic oscillator, we know what its eigenvalue is. Let us consider the ground state. We integrate the Schrödinger equation with the eigenvalue set to be $a = 0.9$, slightly below 1, which we know to be the actual eigenvalue, and we calculate the value of the its first derivative at the origin and we call it α. Then, we integrate the Schrödinger equation with the eigenvalue set to be $b = 1.0$, and we calculate the value of the its first derivative at the origin and we store it as β. If α and β have different signs, we know that the zero of the first derivative is somewhere between a and b. If it turns

out that α and β have the same signs, then we shift $a = 1.0$ and $b = 1.1$ and shoot and compare α and β again. We repeat the process until we find the correct a and b such that a zero of the wave function derivative lies between a and b. For the unperturbed state (g=0), $a = 0.9$ and $b = 1.0$, so we know that the eigenvalue lies within that range. Next, we let $a = 0.90$ and $b = 0.91$. We shoot and then compare α and β. If they differ in sign (which they should not), we will know that the eigenvalue lies between 0.90 and 0.91. If they have the same sign, we increase a to 0.91 and b to 0.92 and shoot and compare α and β again. We repeat this process until we have found the eigenvalue accurate up to two decimal places. We can repeat this process until we have found the eigenvalue for a certain value of g accurate to a specified number of decimal places. We illustrate the shooting method on the simple harmonic oscillator below.

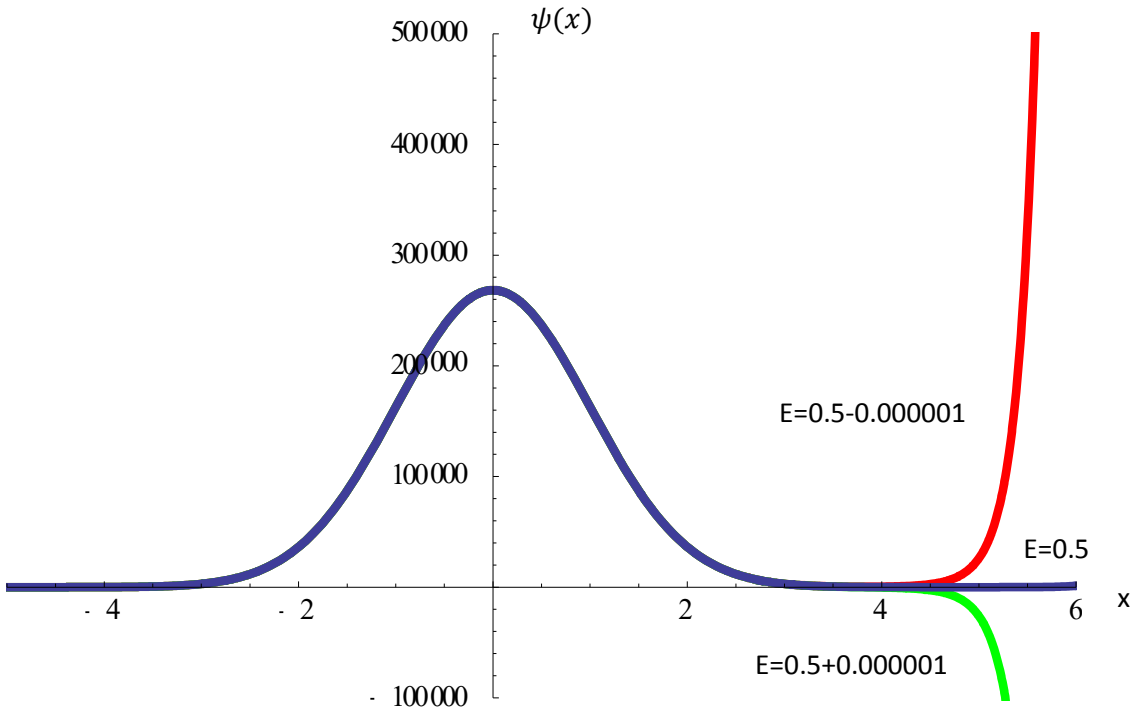


Fig 9: Plot of wave function when doing shooting method for the simple harmonic oscillator. Instead of requiring the wave function to have a zero derivative at the origin, we integrate directly from $x = -5$ to $x = 5$ and require that the wave function vanish exponentially at $x = 5$. If the energy value E is off by even a small value, the wave function will not decay in the manner it is supposed to at the end $x = 5$. In fact, they will diverge very quickly at $x = 5$. The sensitivity of the wave function to the guessed eigenvalue illustrates the accuracy of the method.

After we find the ground state eigenvalue at $E = 1.00$, we can continue scanning for more eigenvalues for $g = 0$ by increasing the values of a and b.

Once we have found the eigenvalue for $g = 0$, we increase g to 0.1. We then repeat the process and scan for all the eigenvalues at that value of g below a certain value for E. The whole process can be repeated to give us the eigenvalues for a desired range of g and E.

Below is the plot of the eigenvalues found by the shooting method for $n = 0$ to $n = 5$.

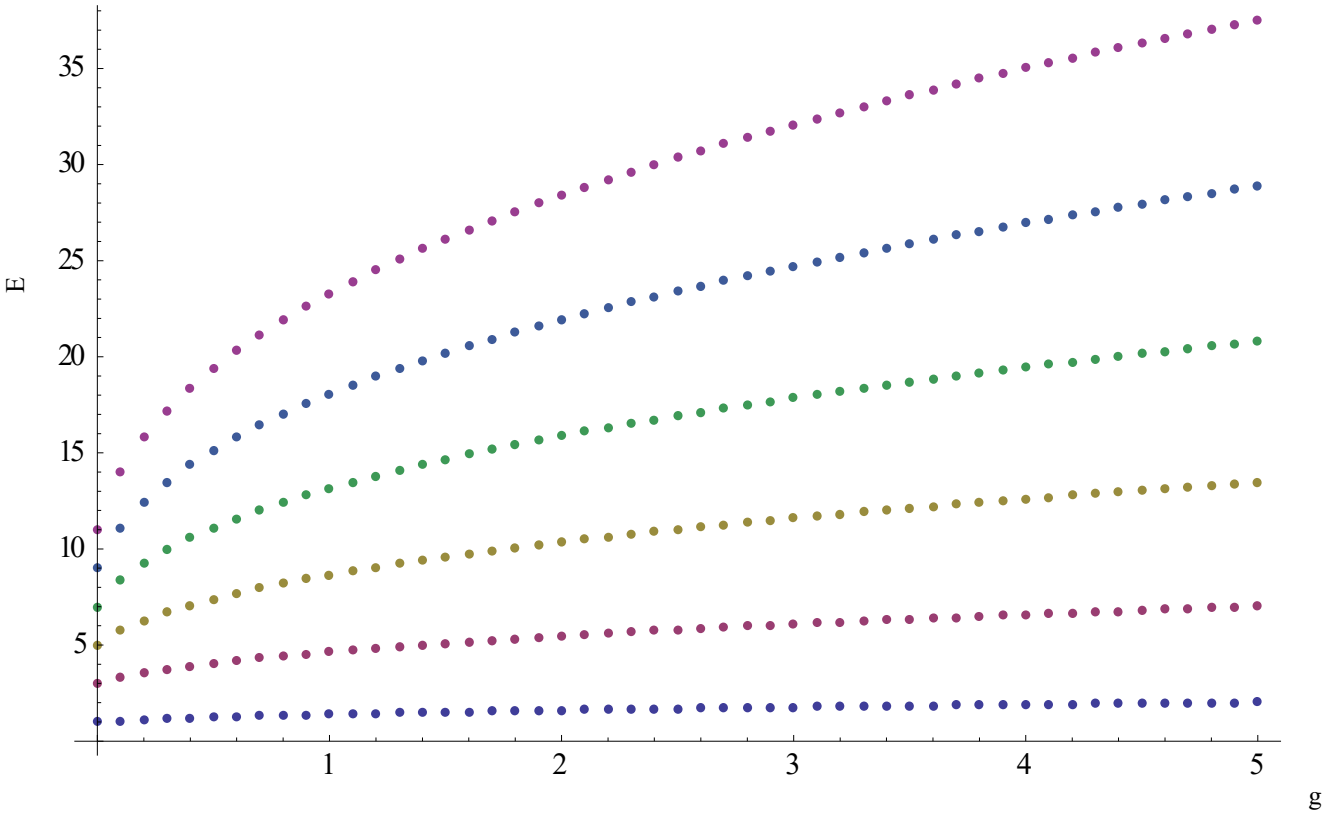


Fig 10: Eigenvalues of $x^2 + gx^4$ potential obtained using the shooting method for the first six energy levels

We compare this with the eigenvalues found using perturbation theory in the plot on the next page.

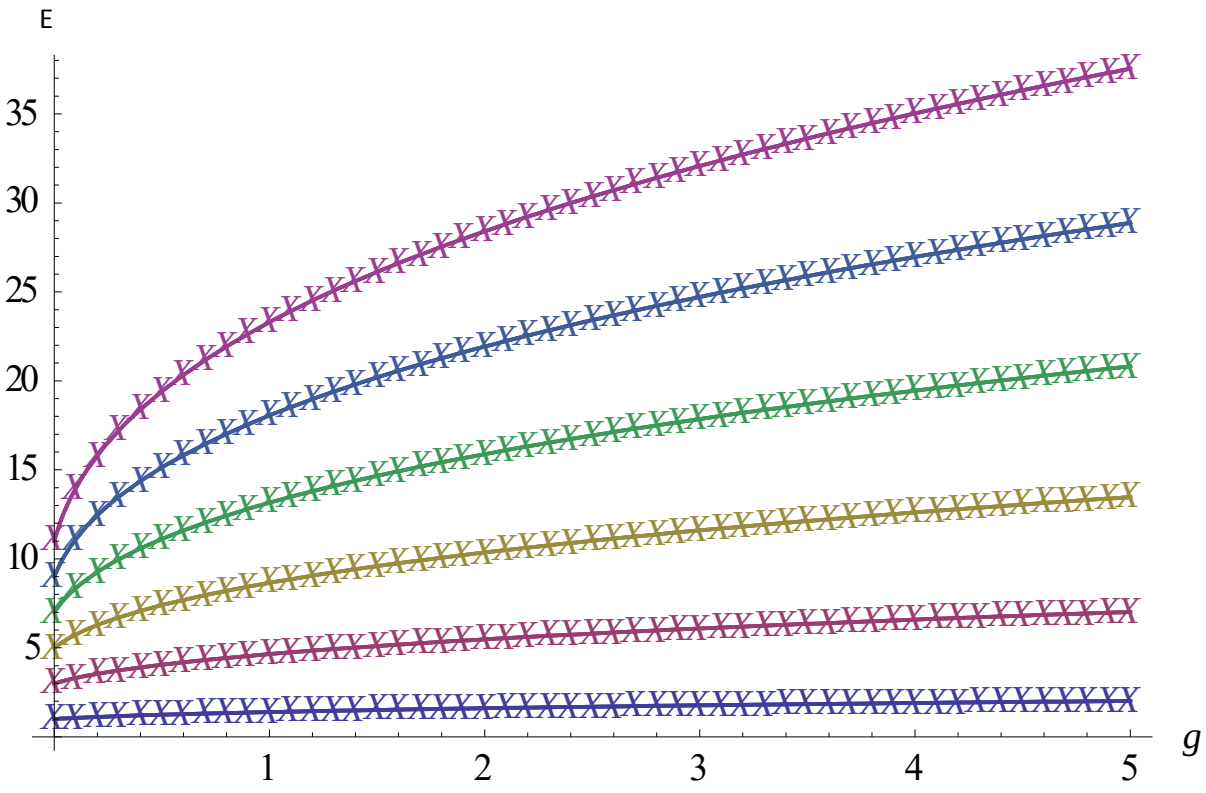


Fig 11: Comparison of the eigenvalues of $x^2 + gx^4$ potential obtained using perturbation theory and the shooting method for the first six energy levels. The lines are the results obtained using perturbation theory while the "X" are obtained by shooting.

We note that for the values of g for which the shooting was done, the Padé approximant matches the numbers calculated using the shooting method very well. Since both methods agree, we conclude that the eigenvalues calculated are accurate.

# 4. The Complex Cubic Perturbation

The previous Hamiltonian we tackled was $\mathcal{PT}$ -symmetric, but it was also Hermitian. Next, we consider a $\mathcal{PT}$ -symmetric non-Hermitian Hamiltonian.

$$H = \hat{p}^2 + \hat{x}^2 + ig\hat{x}^3 \tag{4.1}$$

This is non-Hermitian because when we take the adjoint, the $igx^3$ term gains a minus sign because of $i$. It is still $\mathcal{PT}$ -symmetric because the *T* operator causes the $i$ term to gain a factor of -1 but the *P* operator causes each x to gain a factor of -1 as well, so there is no overall sign change. Furthermore, we will impose a $\mathcal{PT}$ symmetric boundary condition, which we will discuss in greater detail later. The combination of a $\mathcal{PT}$ symmetric operator and a $\mathcal{PT}$ symmetric boundary condition give rise to what we call a $\mathcal{PT}$ symmetric eigenvalue problem.

## 4.1 Perturbation Theory

The time-independent Schrödinger equation for this Hamiltonian is

$$\left(-\frac{d^2}{dx^2} + x^2 + igx^3\right)\psi(x) = E\psi(x) \tag{4.2}$$

This time round, the wave function does not have a parity because referring to equation (3.15), if we replaced x with –x, we will not get back the same equation because the H' term contains $x^3$. So, we have to expand the perturbed wave function in all orders of x up to the maximum order needed. As before, we factor out the exponential term the way we did in (3.3) and we substitute the same series for the perturbed energy and wave function as in (3.6) and (3.7). The unperturbed energy and wave function $A_0$ and $B_0$ are the same as before, and the Schrödinger equation becomes

$$\begin{aligned}\sum_{r=0}^{\infty} g^r\left(-B_r''(x) + 2xB_r'(x) + B_r(x)\right) + i\sum_{r=1}^{\infty} g^r x^3 B_{r-1}(x) \\ = \sum_{r=0}^{\infty}\sum_{s=0}^{r} g^r A_{r-s}B_s(x)\end{aligned} \tag{4.3}$$

For $r \geq 1$, we get

$$-B_r''(x) + 2xB_{\mathrm{r}}'(x) - 2nB_r(x) + ix^3 B_{r-1}(x) = A_r B_0(x) + \sum_{s=1}^{r-1} A_{r-s}B_s(x) \tag{4.4}$$

Note that (4.4) holds for all n. Repeating our previous arguments, the $B_r(x)$ are polynomials of degree $3r + n$. So,

$$B_r(x) = \sum_{j=0}^{3r+n} x^j B_{r,j} \tag{4.5}$$

$$B_r''(x) = \sum_{j=2}^{3r+n} j(j-1)x^{j-2} B_{r,j} \tag{4.6}$$

We then obtain from (4.4)

$$-\sum_{j=0}^{3r+n-2} (j+2)(j+1)x^j B_{r,j+2} + \sum_{j=1}^{3r+n} (2j-2n)x^j B_{r,j} + i\sum_{j=3}^{3r+n} x^j B_{r-1,j-3} - 2nB_{r,0} = A_r \sum_{j=0}^{n} B_{0,j}x^j + \sum_{j=0}^{3r+n} x^j \sum_{s=1}^{r-1} A_{r-s}B_{s,j} \tag{4.7}$$

Where the last sum on the right hand side vanishes for r=1. If we obtained the recursion relations from the coefficient of each power of x from (3.18) directly, we would have to take into consideration that some terms are present and some terms are not for each value of n and r. We can deal with this by defining

$$B_{r,j} = 0 \qquad \text{for } j < 0 \tag{4.8}$$

Then, we can extend the lower limit of the third sum of the left hand side to $j = 1$. Because of this, we have to treat the $n = 0$ case separately. For $n = 0$, we get

$$-2B_{r,2} = A_r + \sum_{s=1}^{r-1} A_{r-s}B_{s,0} \tag{4.9}$$

$$for\ j = 1,2,\dots,3r-2$$

$$-(j+2)(j+1)B_{r,j+2} + (2j-2n)B_{r,j} + iB_{r-1,j-3} = \sum_{s=1}^{r-1} A_{r-s}B_{s,j} \tag{4.10}$$

$$(2j-2n)B_{r,j} + iB_{r-1,j-3} = \sum_{s=1}^{r-1} A_{r-s}B_{s,j} \qquad for\ j = 3r-1, 3r \tag{4.11}$$

Where the sums on the right hand side disappear for $r = 1$. Note that $B_{r,0}$ terms are undetermined. This is because we have the freedom to subtract any multiple of $H_0$ (zeroth order Hermite polynomial) from the wave function. For $n \geq 1$,

$$-2B_{r,2} = A_r + \sum_{s=1}^{r-1} A_{r-s}B_{s,0} \tag{4.12}$$

$$for\ j = 1,2,\dots,3r-2$$

$$-(j+2)(j+1)B_{r,j+2} + (2j-2n)B_{r,j} + iB_{r-1,j-3} = A_r + \sum_{s=1}^{r-1} A_{r-s}B_{s,j} \tag{4.13}$$

Where the $A_r$term on the right hand side vanishes if $j > n$.

$$(2j-2n)B_{r,j} + iB_{r-1,j-3} = \sum_{s=1}^{r-1} A_{r-s}B_{s,j} \qquad for\ j = 3r-1,3r \tag{4.14}$$

The perturbation series for the energy are then calculated using Mathematica and they are listed below:

$$E_0 = 1 + \frac{11}{16}g^2 - \frac{465}{256}g^4 + \frac{39709}{4096}g^6 - \frac{19250805}{262144}g^8 + \frac{2944491879}{4194304}g^{10} - \frac{1075012067865}{134217728}g^{12} + \cdots \tag{4.15}$$

$$E_1 = 3 + \frac{71}{16}g^2 - \frac{5625}{256}g^4 + \frac{827539}{4096}g^6 - \frac{649176885}{262144}g^8 + \frac{152513050809}{4194304}g^{10} - \frac{81681198068025}{134217728}g^{12} + \cdots \tag{4.16}$$

$$E_2 = 5 + \frac{191}{16}g^2 - \frac{23475}{256}g^4 + \frac{5181319}{4096}g^6 - \frac{5929555695}{262144}g^8 + \frac{1983833350149}{4194304}g^{10} - \frac{1480895068749675}{134217728}g^{12} + \cdots \tag{4.17}$$

$$E_3 = 7 + \frac{371}{16}g^2 - \frac{62475}{256}g^4 + \frac{18657289}{4096}g^6 - \frac{28547953455}{262144}g^8 + \frac{12629014122459}{4194304}g^{10} - \frac{12335622660979275}{134217728}g^{12} + \cdots \tag{4.18}$$

$$E_4 = 9 + \frac{611}{16}g^2 - \frac{131085}{256}g^4 + \frac{49589809}{4096}g^6 - \frac{95572832985}{262144}g^8 + \frac{52955574390579}{4194304}g^{10} - \frac{64434150590988285}{134217728}g^{12} + \cdots \quad 4.19$$

$$E_5 = 11 + \frac{911}{16}g^2 - \frac{237765}{256}g^4 + \frac{109091359}{4096}g^6 - \frac{254205912345}{262144}g^8 + \frac{169769670576429}{4194304}g^{10} - \frac{248205956703612765}{134217728}g^{12} + \cdots \quad 4.20$$

$$E_6 = 13 + \frac{1271}{16}g^2 - \frac{390975}{256}g^4 + \frac{211052539}{4096}g^6 - \frac{577534523475}{262144}g^8 + \frac{452087065979409}{4194304}g^{10} - \frac{773240779139026575}{134217728}g^{12} + \cdots \quad 4.21$$

It is interesting to note that the odd terms are missing, but and the terms alternate in sign. This is the reason why the eigenvalues are real. We show the Schrödinger equation again.

$$H = p^2 + x^2 + igx^3 \quad 4.22$$

We can view $ig$ as the perturbation parameter rather than *g.* Then, then the perturbed eigenvalues and wave functions will be power series in terms of $ig$. Then, the odd order terms will be imaginary. We know that when g is zero, we obtain the simple harmonic oscillator. Comparison with the shooting method will show that the eigenvalues remain real for small values of g as well. Thus, the eigenvalue perturbation series must be real, and so the odd order terms must vanish.

The perturbation series contains the first 200 corrections, and as before, we convert them into Padé approximants.

The plots of the Padé approximants are shown below:

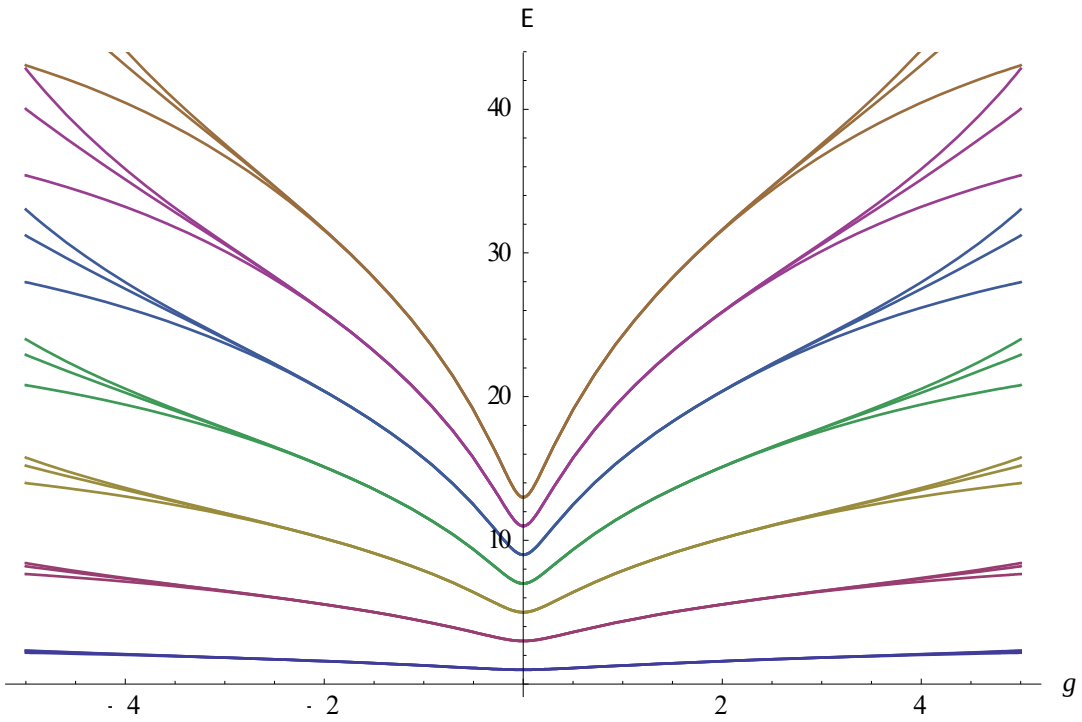


Fig 12: Padé approximant for the eigenvalues perturbation series of $x^2 + igx^3$ potential for g=-5 to g=5. For each energy level, the highest most graph corresponds to (99,101) Padé, the second highest corresponds to (101,99) and the lowest graph corresponds to (100,100)

Note that the graphs are even with respect to g. This is because the Hamiltonian is $\mathcal{PT}$ -symmetric.

This time round, the Padé approximants are valid in a region much smaller than the previous potential. Below is a table containing estimates for the largest g for which the Padé approximants are valid.

| n | g |
|---|---|
| 0 | 5.0±0.5 |
| 1 | 3.5±0.5 |
| 2 | 3.0±0.5 |
| 3 | 2.5±0.5 |
| 4 | 2.5±0.5 |
| 5 | 2.0±0.5 |

Table 2: Approximate maximum values of g for which the Padé approximant is valid

## 4.2 Shooting Method

Next we use the shooting method to calculate the eigenvalues. We proceed as before, but the ratio of the first derivative of the wave function to the wave function is:

$$\psi'(-10) = -\frac{2x(x^2 - E) + 3g^2x^5}{4[(x^2 - E)^2 + g^2x^6]} + ((x^2 - E)^2 + g^2x^6)^{\frac{1}{4}} \qquad 4.23$$

Also, because the wave functions do not have parity, we have to integrate (4.2) from -10 to 10 and see if the wave function vanishes at $x = 10$. The eigenvalues found are plotted below.

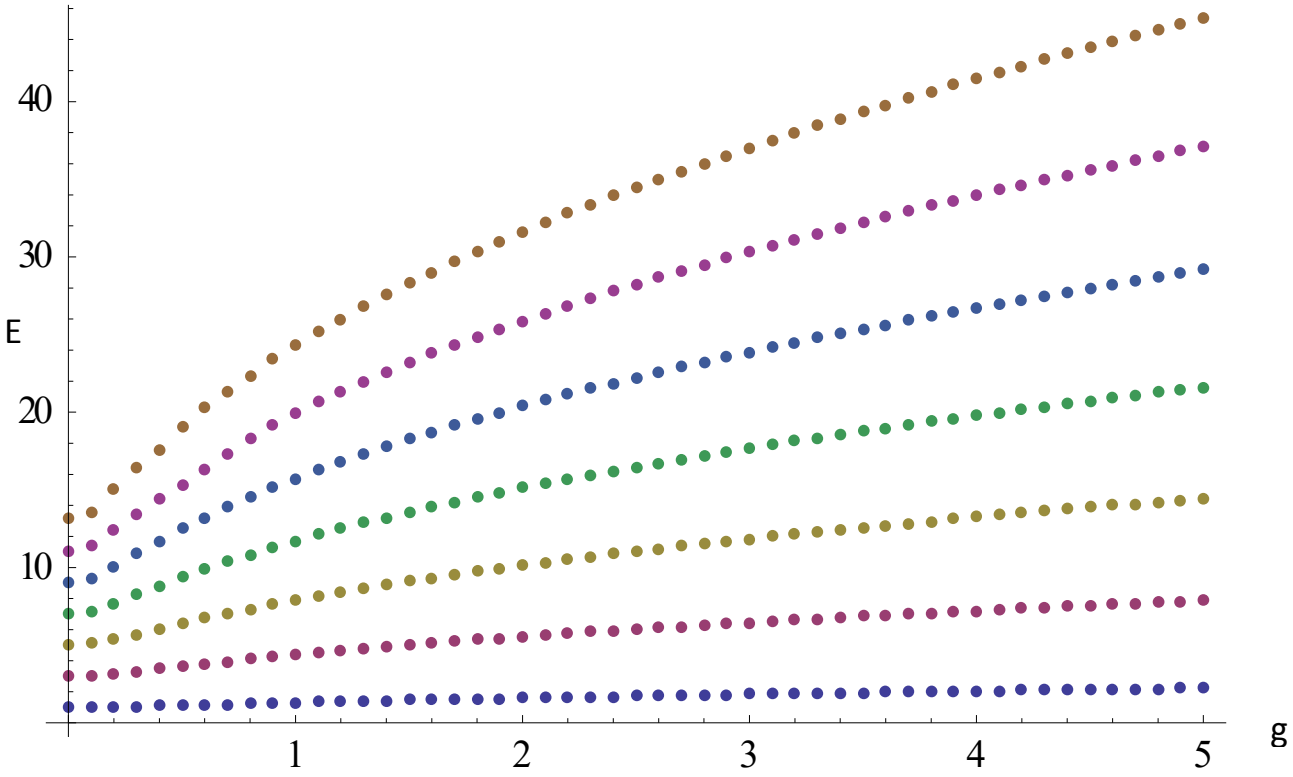


Fig 13: Eigenvalues of $x^2 + igx^3$ potential obtained using the shooting method for the first six energy levels

We then compare this with the Padé approximants.

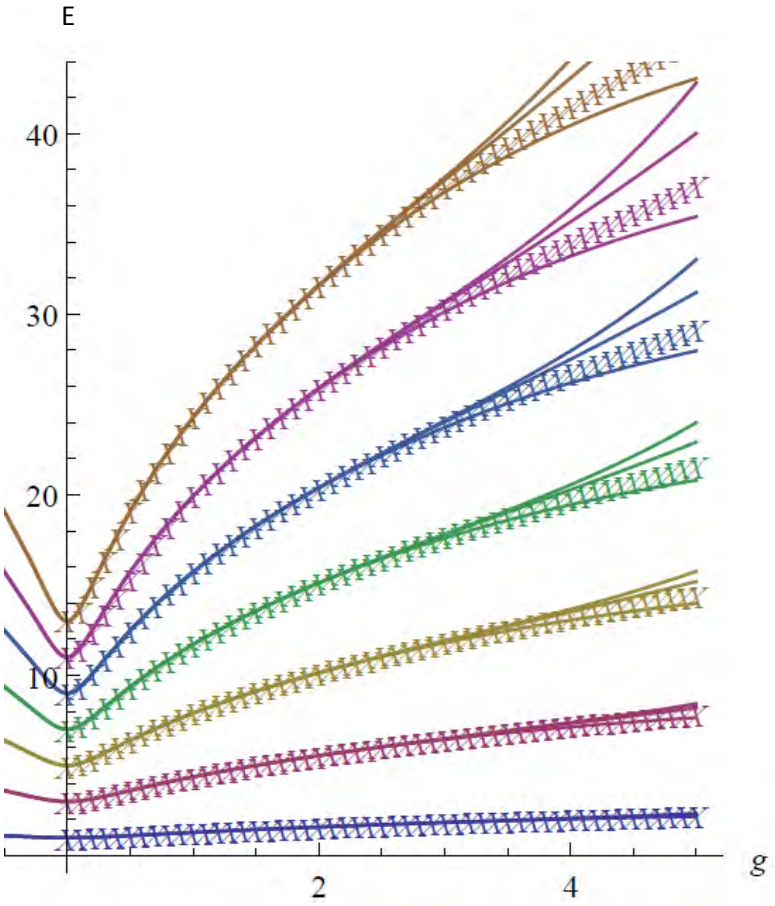


Fig 14: Comparison of the eigenvalues of $x^2 + igx^3$ potential obtained using perturbation theory and the shooting method for the first six energy levels. The lines are obtained by using perturbation theory while the "X' are obtained by using the shooting method. Since the perturbation series is even in g, we show the part for the non-negative values of g

We see that the results obtained from perturbation theory and the shooting method match up. In fact, when the Padé approximants for each energy level split up, the values obtained from the shooting method seem to be the average of them. We conclude that the two methods agree very well with each other.

## 4.3 Shooting on the Complex Plane

Since (4.2) is a complex differential equation, we can try to shoot it on the complex plane. This is known as an analytic continuation of an eigenvalue problem, and it is discussed in [8].

First, we have to determine the region for which we can do the shooting. We do this by examining the WKB approximation.

For large values of x, we get

$$V - E \sim igx^3 \tag{4.24}$$

Then,

$$\psi_{WKB}(x) = \frac{A}{(igx^3)^{\frac{1}{4}}} e^{\pm \int^x \sqrt{igx'^3}dx'} \tag{4.25}$$

Where A is a constant. Next, we find the roots in the expression.

$$\sqrt{igx^3} = \sqrt{g} r^{\frac{3}{2}} e^{i(\frac{3\theta}{2}+\frac{\pi}{4})} \tag{4.26}$$

$$(igx^3)^{\frac{1}{4}} = g^{\frac{1}{4}} r^{\frac{3}{4}} e^{i(\frac{3\theta}{4}+\frac{\pi}{8})} \tag{4.27}$$

Since we are working with the differential equation on the complex plane, let us use the letter “z” instead of “x”. The wave function becomes

$$\psi(r,\theta)_{WKB} = \frac{A}{g^{\frac{1}{4}} r^{\frac{3}{4}} e^{i(\frac{3}{4}\theta+\frac{\pi}{8})}} e^{\pm\frac{2}{5} r^{\frac{5}{2}} \sqrt{g} e^{i(\frac{5\theta}{2}+\frac{\pi}{4})}} \tag{4.28}$$

There are two wave functions we can use. Let us stick to the wave function with the minus sign in from of the $\frac{2}{5}$ factor. Now, to obtain a solution that vanishes at infinity, we need the real part of the exponent to be negative, so the cosine term must be positive. So, we get the following inequality.

$$-\frac{\pi}{2} \leq \frac{\pi}{4} + \frac{5\theta}{2} \leq \frac{\pi}{2} \tag{4.29}$$

$$-\frac{3\pi}{10} \leq \theta \leq \frac{\pi}{10} \tag{4.30}$$

So, for $Re(z) \geq 0$, we need to integrate within this wedge. Let us integrate along the middle of the wedge, so $\theta = -\frac{\pi}{10}$. For the $Re(z) < 0$ region, we integrate along a path that is the

reflection of the first path about the imaginary axis, so we integrate along $\theta = -\frac{9\pi}{10}$. Below we have a figure that shows the wedge and the integration path. Note that in principle, we do not require the entire integration path to be in those wedges. As long as the integration paths are within the wedges as $|x| \to \infty$, the boundary conditions are satisfied. For simplicity, however, we choose the integration paths to be straight lines, and we pick the lines to be in the middle of the Stokes wedges. That is because in the middle of the wedge, $\frac{\pi}{4} + \frac{5\theta}{2} = 0$, and the real part of the exponent in (4.28) will have its largest magnitude, and thus the wave function will decrease fastest along the middle of the Stokes wedge.

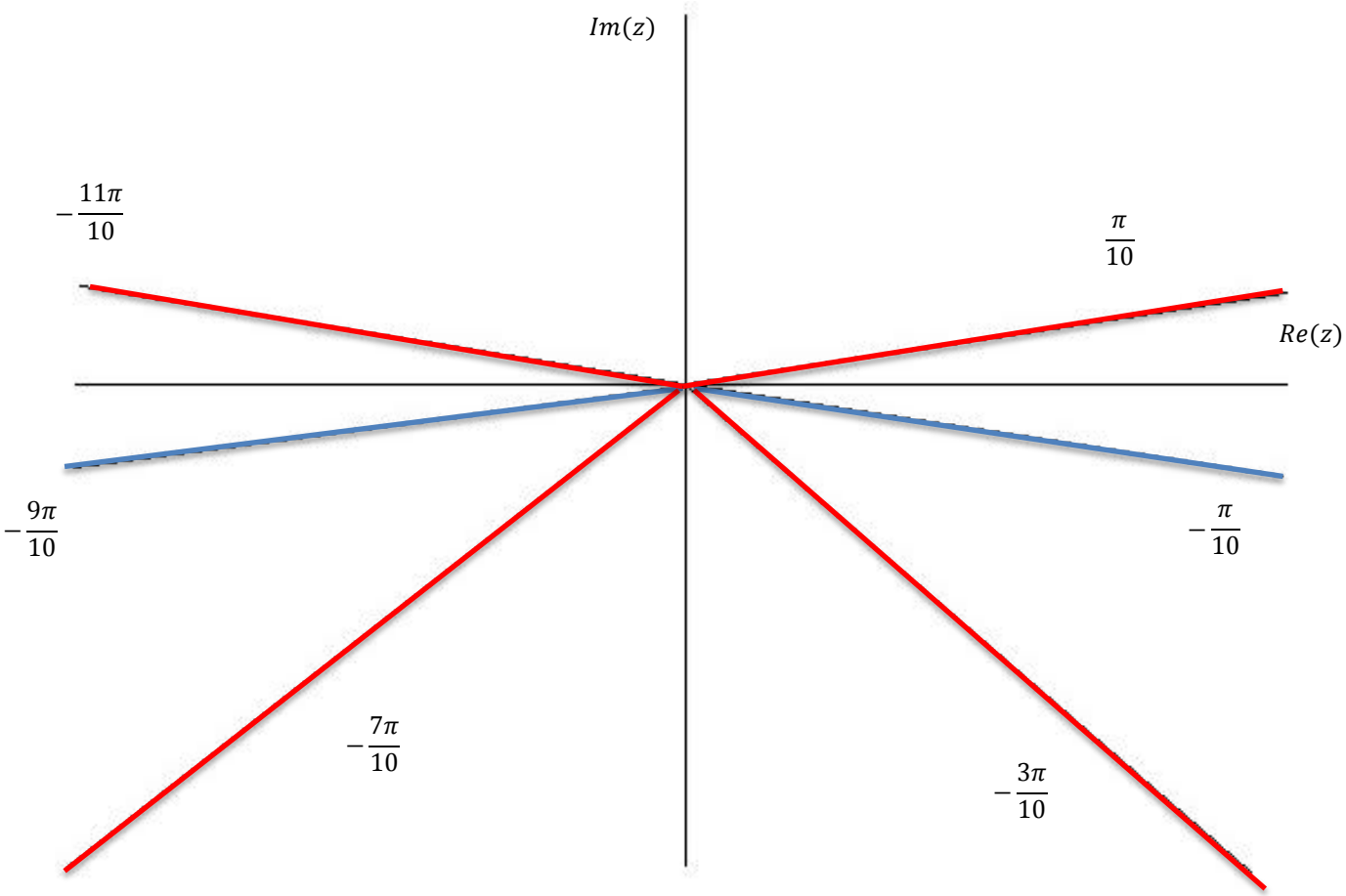


Fig 15: The red lines depict the boundary of wedges while the blue lines are our path of integrations. The symmetry about the imaginary axis is equivalent to $\mathcal{PT}$ symmetry.

The differential equation (4.2) becomes a differential equation for the variable r, since the angle θ is fixed. (4.2) leads to the following equation:

$$e^{-2i\theta}\frac{d^2\phi}{dr^2}(r) + \left[E - \left(r^2 e^{2i\theta} + igr^3 e^{3i\theta}\right)\right]\phi(r) = 0 \qquad 4.31$$

Now, the boundary conditions at $\phi(r = 10)$ is given by differentiating (4.28) with respect to r, and dividing by (4.28). By setting $\psi_{WKB}(10) = 1$, we obtain

$$\phi(r)'_{WKB} = -\frac{7}{4r} \pm \sqrt{g} r^{\frac{3}{2}} e^{i\left(\frac{5\theta}{2}+\frac{\pi}{4}\right)} \quad 4.32$$

Now, we want the wave functions integrated on both halves of the complex plane to match at the origin. Since they will have different normalisation factors, we cannot simply equate them and their derivatives at the origin. In fact,

$$\psi_L(0^-) = N\tilde{\psi}_R(0^+) \quad 4.33$$

Where we have divided the normalisation constant for $\psi_L$. Here, N is the ratio of their normalisation constants.

Let $\tilde{\psi}_R$ be the wave function on the right half-plane obtained numerically, and let $\psi_R$be the wave function on the right that has the correct factor such that it will match $\psi_L$. So,

$$\psi_R = N\tilde{\psi}_R \quad 4.34$$

$$\psi_L(z) = \psi_R(z) \quad 4.35$$

Then, we get

$$\frac{d\psi_L(z)}{dz_L} = \frac{d\psi_R(z)}{dz_R} \quad 4.36$$

Let $z_L = re^{i\theta_L}$, $z_R = re^{i\theta_R}$, where $\theta_L = -\frac{9\pi}{10}$, $\theta_R = -\frac{\pi}{10}$.

Then, (4.39) becomes

$$\phi_L{}'(r) = e^{i(\theta_L - \theta_R)}\phi_R{}'(r) \quad 4.37$$

Where $\psi(z) = \phi(r)$. We can then obtain the following boundary condition.

$$\frac{\phi_L'(0^-)}{\phi_L(0^-)} = e^{-\frac{i4\pi}{5}} \frac{\widetilde{\phi_R'}(0^+)}{\widetilde{\phi_R}(0^+)} \quad 4.38$$

This will be a boundary condition that the numerically calculated wave functions need to satisfy.

The numerically calculated eigenvalues obtained by shooting off the real axis on the complex plane are shown below.

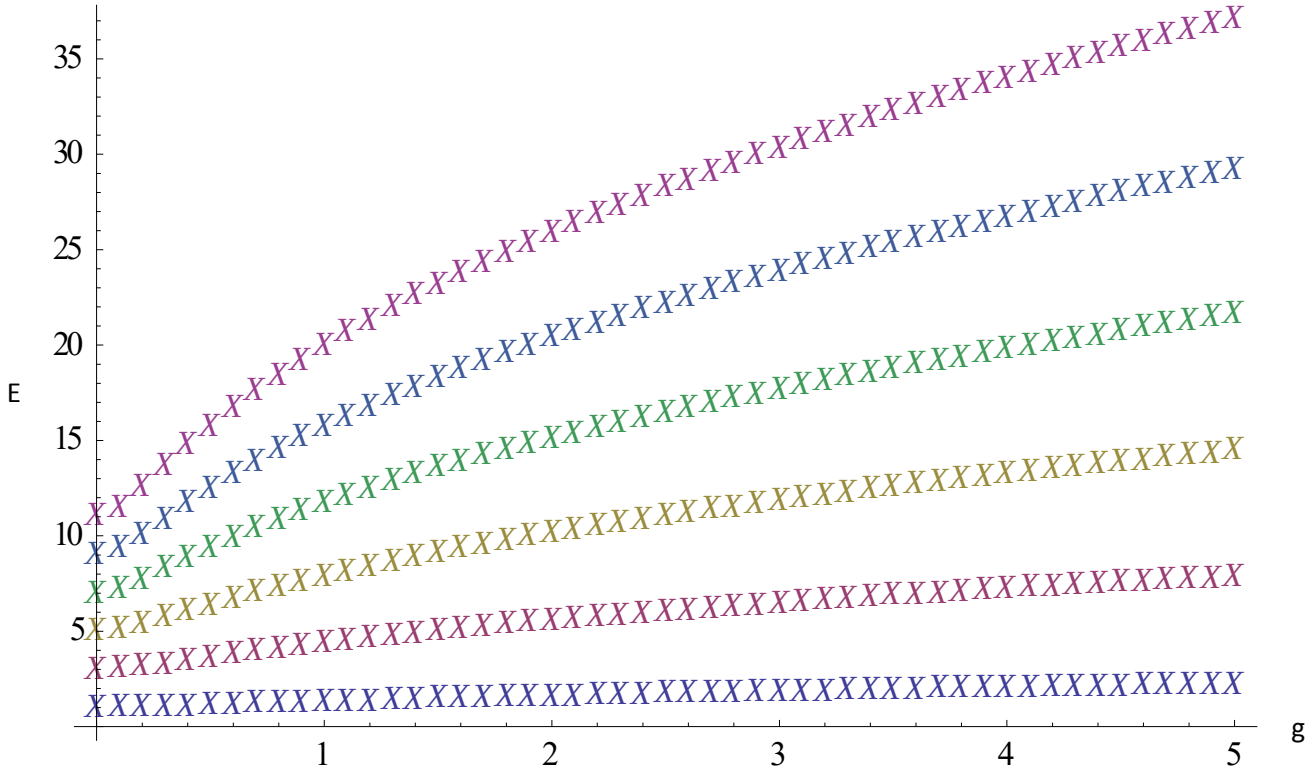


Fig 16: Eigenvalues of $x^2 + igx^3$ potential obtained using the shooting method on the complex plane for the first six energy levels

Now, we compare this with our previous result that was done by doing the shooting on the real line.

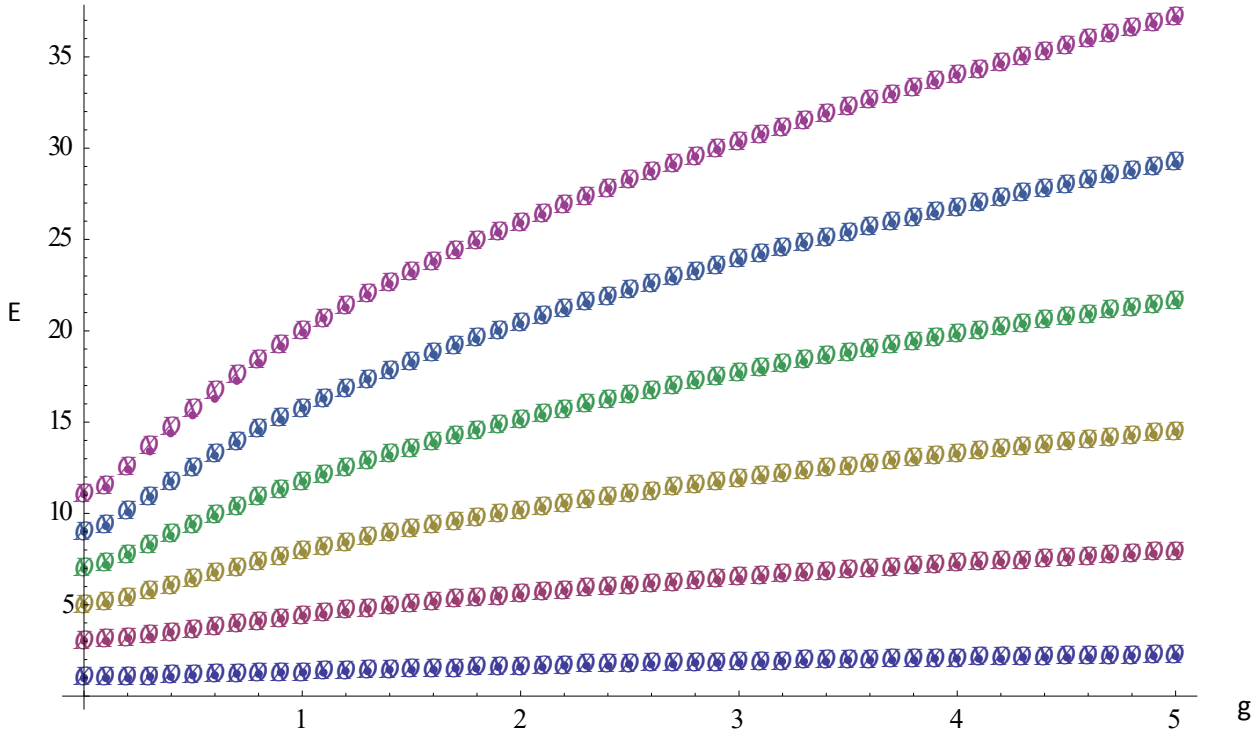


Fig 17: Comparison of the eigenvalues of $x^2 + igx^3$ potential obtained using the shooting method for the first six energy levels on both the real line and on the complex plane. The "X" are the results obtained by complex shooting while the "O" are obtained by shooting on the real line

From the figure, we can see that the eigenvalues obtained using both shooting methods match up. Therefore, the shooting performed on the complex plane is valid. The reason for this is that referring to figure 10, we see that both paths of integration (the real axis and the one off the real axis) lie in the same wedge. Thus, both eigenvalue problems are actually the same and yield the same eigenvalues.

# 5. The Complex Quintic Perturbation

Now we take a look at the following Hamiltonian.

$$H = \hat{p}^2 + \hat{x}^2 - ig\hat{x}^5 \tag{5.1}$$

The resulting differential equation is

$$\left(-\frac{d^2}{dx^2} + x^2 - igx^5\right)\psi(x) = E\psi(x) \tag{5.2}$$

## 5.1 Perturbation Theory

Proceeding as before, we obtain the following recursion relations:

$$-(j+1)(j+2)B_{r,j+2} + (2j-2n)B_{r,j} = A_r B_{0,j} + \sum_{s=1}^{r-1} A_{r-s}B_{s,j} \qquad for\ j = 0,1,2,3,4 \tag{5.3}$$

Where the first term on the left hand side vanishes if $j > 5r + n - 2$. The first term on the right hand side vanishes if $j > n$. The second recursion relation is

$$-(j+1)(j+2)B_{r,j+2} + (2j-2n)B_{r,j} + iB_{r-1,j-5} = A_r B_{0,j} + \sum_{s=1}^{r-1} A_{r-s}B_{s,j} \tag{5.4}$$

$$for\ j = 5, \dots, 5r + n - 2\ (n \geq 2)$$

Where the first term on the right hand side vanishes if $j > n$. Lastly, we have

$$(2j-2n)B_{r,j} + iB_{r-1,j-5} = \sum_{s=1}^{r-1} A_{r-s}B_{s,j} \qquad for\ j = 5r + n - 1, 5r + n \tag{5.5}$$

Where the second term on the left hand side vanishes if $j < 5$.

The perturbation series is found to be

$$E_0 = 1 + \frac{449}{64}g^2 - \frac{1723225}{1024}g^4 + \frac{928230645}{512}g^6 - \frac{21855598127812155}{4194304}g^8 + \frac{4241564049337820159267}{134217728}g^{10} - \frac{3004018902075901935125903275}{8589934592}g^{12} + \cdots \tag{5.6}$$

$$E_1 = 3 + \frac{5769}{64}g^2 - \frac{55978965}{1024}g^4 + \frac{1726220827845}{16384}g^6 - \frac{1837895347604862315}{4194304}g^8 + \frac{458431674897151341746757}{134217728}g^{10} - \frac{3918012428231092286688779301 15}{8589934592}g^{12} + \cdots \quad (5.7)$$

$$E_2 = 5 + \frac{31529}{64}g^2 - \frac{725013275}{1024}g^4 + \frac{42510385518555}{16384}g^6 - \frac{71767789598896864725}{4194304}g^8 + \frac{24655643588409939496522577}{134217728}g^{10} - \frac{26384964228947106683981642362325}{8589934592}g^{12} + \cdots \quad (5.8)$$

$$E_3 = 7 + \frac{107969}{64}g^2 - \frac{5205697735}{1024}g^4 + \frac{282306040675335}{8192}g^6 - \frac{1567714101856010790885}{4194304}g^8 + \frac{791759677111410484076413007}{134217728}g^{10} - \frac{1128084691762456704445372850663485}{8589934592}g^{12} + \cdots \quad (5.9)$$

$$E_4 = 9 + \frac{280449}{64}g^2 - \frac{25235908425}{1024}g^4 + \frac{2377372219113645}{8192}g^6 - \frac{21359860254281050296795}{4194304}g^8 + \frac{162071512018985963473667767}{134217728}g^{10} - \frac{32149763011375712936070920485812675}{8589934592}g^{12} + \cdots \quad (5.10)$$

$$E_5 = 11 + \frac{609449}{64}g^2 - \frac{93231879125}{1024}g^4 + \frac{28601440784556615}{16384}g^6 - \frac{200216154841372798637355}{4194304}g^8 + \frac{225840319621430069032895577017}{134217728}g^{10} - \frac{63254940079177067371010958396292 6475}{8589934592}g^{12} + \cdots \quad (5.11)$$

$$E_6 = 13 + \frac{1170569}{64}g^2 - \frac{283146505915}{1024}g^4 + \frac{133628320215875145}{16384}g^6 - \frac{139886467017838759895176 5}{4194304}g^8 + \frac{228866288816994334218124632 1757}{134217728}g^{10} - \frac{898670395290755714912081384945926 7965}{8589934592}g^{12} + \cdots \quad 5.12$$

$$E_7 = 15 + \frac{2054529}{64}g^2 - \frac{742540303575}{1024}g^4 + \frac{128520562454221545}{4096}g^6 - \frac{774554110772077070293792 5}{4194304}g^8 + \frac{178681637385674515059205055688 27}{134217728}g^{10} - \frac{966903771956468786933138966160358607 25}{8589934592}g^{12} + \cdots \quad 5.13$$

$$E_8 = 17 + \frac{3367169}{64}g^2 - \frac{1738356714185}{1024}g^4 \frac{424330022970404655}{4096}g^6 - \frac{355871503512757712845078 35}{4194304}g^8 + \frac{112617580767088329163325095370507}{134217728}g^{10} - \frac{822819631183036157876537275104276397835}{8589934592}g^{12} + \cdots \quad 5.14$$

$$E_9 = 19 + \frac{5229449}{64}g^2 - \frac{3718893468325}{1024}g^4 + \frac{4955782430315884065}{16384}g^6 - \frac{140446955069497643689501995}{4194304}g^8 + \frac{594570628580589313989104841577517}{134217728}g^{10} - \frac{574577513353644255632917115815566434387 5}{8589934592}g^{12} + \cdots \quad 5.15$$

$$E_{10} = 21 + \frac{7777449}{64}g^2 - \frac{7394461699275}{1024}g^4 + \frac{13083803358884155215}{16384}g^6 - \frac{488798454990011628629678805}{4194304}g^8 + \frac{270694443954678817254345938367 1017}{134217728}g^{10} - \frac{339350254987097313567687858785970751919 25}{8589934592}g^{12} + \cdots \quad 5.16$$

$$E_{11} = 23 + \frac{11162369}{64}g^2 - \frac{13839224510615}{1024}g^4 + \frac{158825590410929087 85}{8192}g^6 - \frac{153096058458816084163716 4965}{4194304}, g^8 + \frac{108740031770077594829997835 10188007}{134217728}g^{10} - \frac{173734132470095764699701088337800256797565}{8589934592}g^{12} + \cdots \quad 5.17$$

The Padé approximants are then calculated and plotted in the figure below.

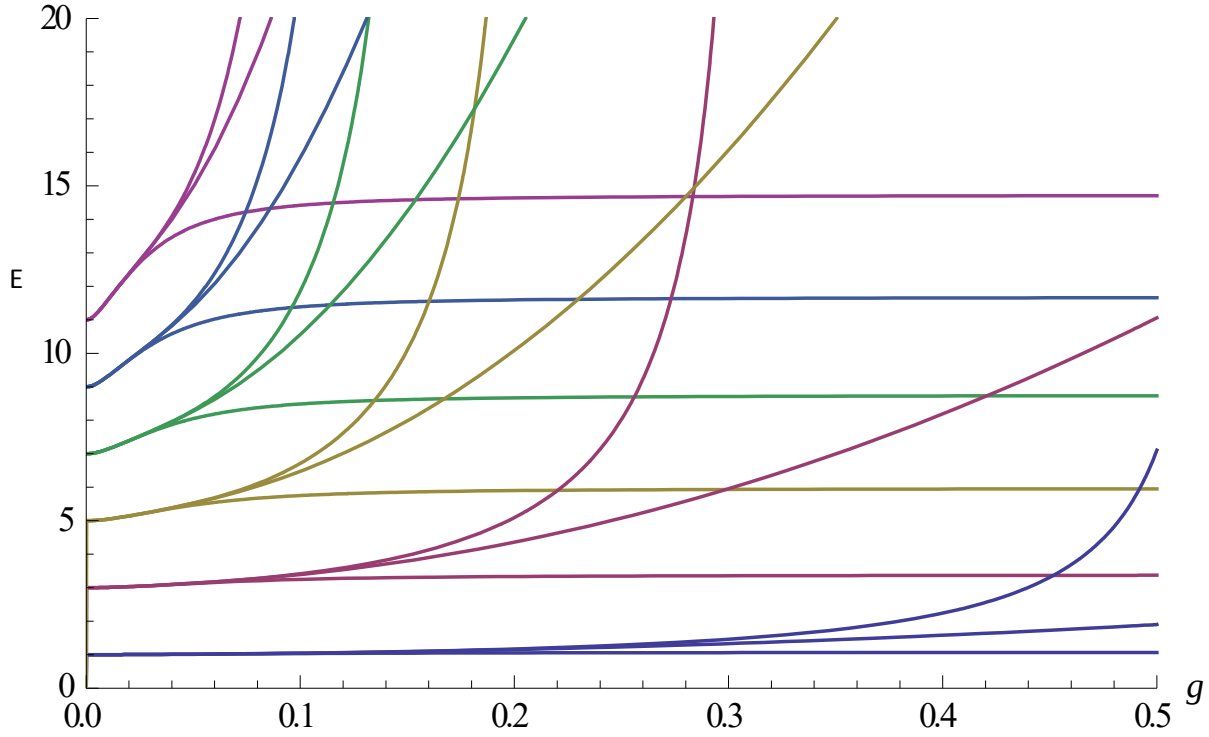


Fig 18: Padé approximant for the eigenvalues perturbation series of $x^2 - igx^5$ potential for g=0 to g=0.5. For each energy level, the highest most graph corresponds to (99,101) Padé, the second highest corresponds to (101,99) and the lowest graph corresponds to (100,100).

Note that the region for which the Padé approximants are valid is much smaller than the previous Hamiltonians. An estimate for the maximum value of g for which the Padé approximants are valid is shown below.

| n | g |
|---|---|
| 0 | 0.1±0.04 |
| 1 | 0.06±0.02 |
| 2 | 0.04±0.02 |
| 3 | 0.04±0.02 |
| 4 | 0.04±0.02 |
| 5 | 0.02±0.02 |

Table 2: Maximum values of g for which the Padé approximant is valid

We also computed the perturbation series to the 400$^{th}$ correction and then calculated the (201,199), (200,200) and (199,201) Padé to see the improvement gained from the extra 200 terms. We plot the results below. This time round we calculated up to the 11$^{th}$ excited state.

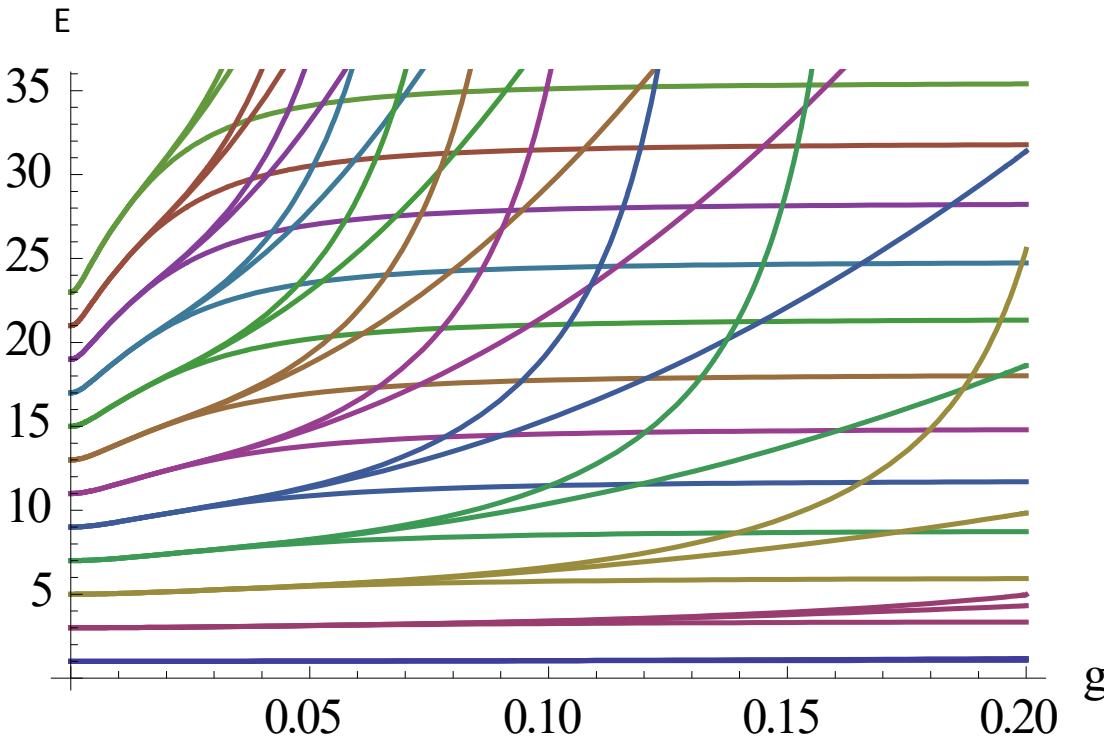


Fig 19: Padé approximant for the eigenvalues perturbation series of $x^2 - igx^5$ potential for g=0 to g=0.2. For each energy level, the highest most graph corresponds to (199,201) Padé, the second highest corresponds to (201,199) and the lowest graph corresponds to (200,200).

If we compare the values of g for which the Padé approximant is valid, we note that there is very little improvement over the Padé series calculated from 201 terms. This shows that perturbation theory has a limitation of being valid for only small values of the perturbation parameter in this instance. Its validity has to be cross checked with other methods like the shooting method.

## 5.2 Shooting Method

### 5.2.1 Shooting on the real axis

As before, we first perform shooting on the real axis. The eigenvalues obtained by shooting on the real axis are plotted below. We can use (4.37) to obtain the boundary condition at the origin

$$\frac{\phi_L'(0^-)}{\phi_L(0^-)} = -\frac{\widetilde{\phi_R'}(0^+)}{\widetilde{\phi_R}(0^+)} \tag{5.18}$$

Here, $\theta_R = -\pi$, $\theta_L = 0$.

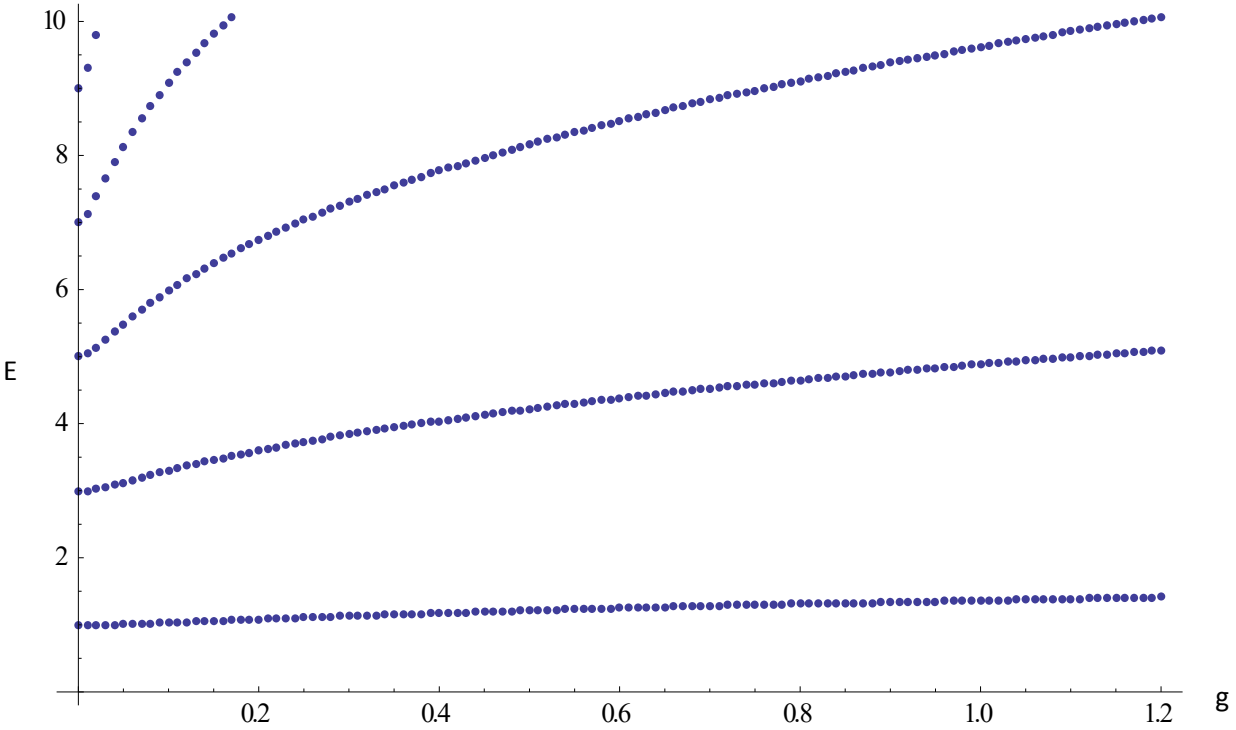


Fig 20: Eigenvalues of $x^2 - igx^5$ potential obtained using the shooting method on the real line up to E=10

### 5.2.2 Shooting off the real axis

Now, we try to perform numerical shooting off the real axis in the same way we did for the complex cubic perturbation. Let us first calculate the wedge for which the wave function goes to zero at infinity. If we repeat the calculations as in section 4.3, we get

$$-\frac{5\pi}{14} \leq \theta \leq -\frac{\pi}{14} \tag{5.19}$$

Let us integrate along the middle of the wedge, so $\theta_R = -\frac{3\pi}{14}$, $\theta_L = -\frac{11\pi}{14}$.

The boundary condition at "infinity" is given by

$$\phi'(r = \pm 10) = -\frac{5}{4r} + \sqrt{g}e^{i\left(\frac{7\theta}{2} - \frac{\pi}{4}\right)}r^{\frac{5}{2}} \qquad 5.20$$

While the boundary condition at the origin is given by

$$\frac{\phi_L'(0^-)}{\phi_L(0^-)} = e^{-\frac{i4\pi}{7}}\frac{\widetilde{\phi_R'}(0^+)}{\widetilde{\phi_R}(0^+)} \qquad 5.21$$

The Stokes Wedges together with the integration paths are shown below.

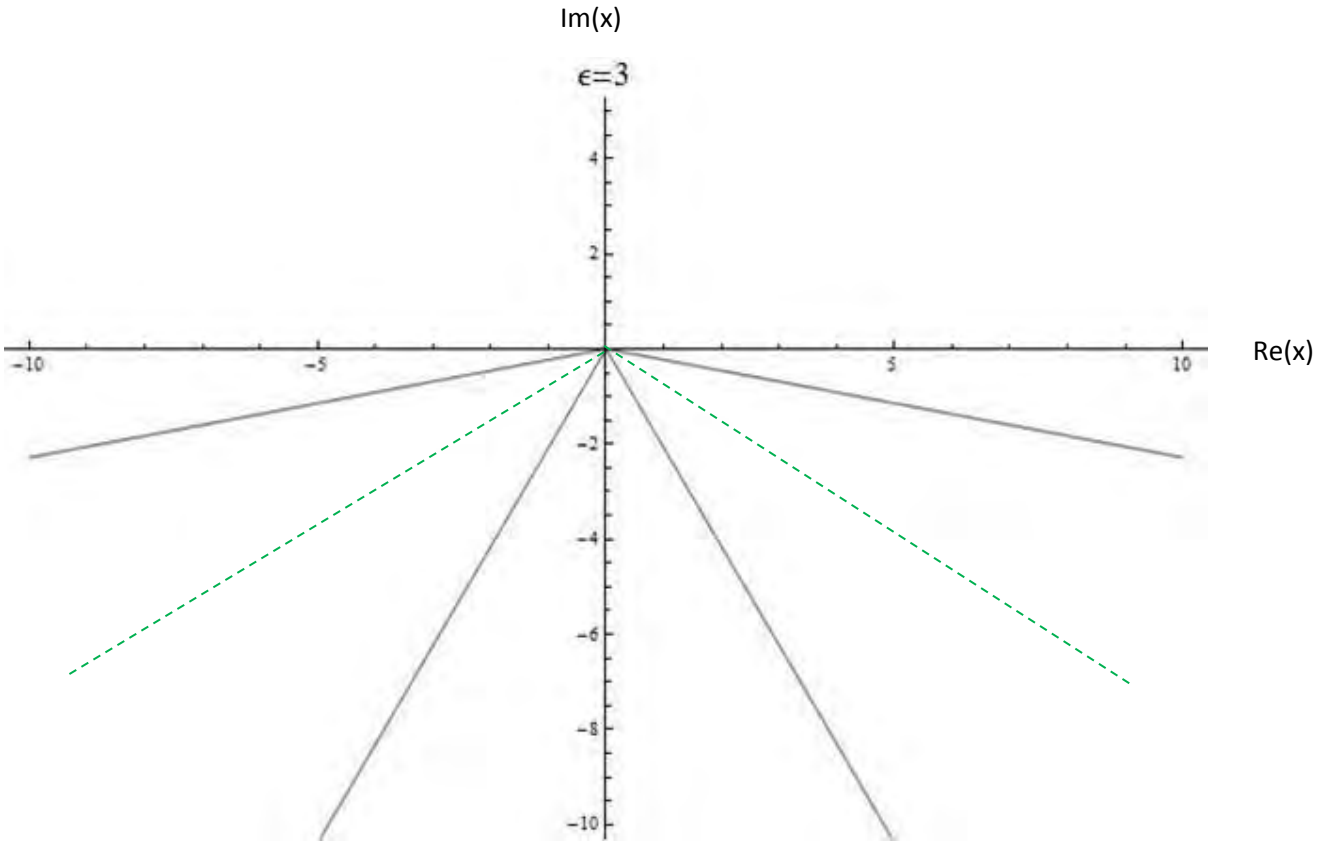


Fig 21: Stokes Wedges for $-igx^5$. The dashed lines are the integration paths while the full lines are the boundaries of the wedges

The eigenvalues obtained are plotted in a graph below.

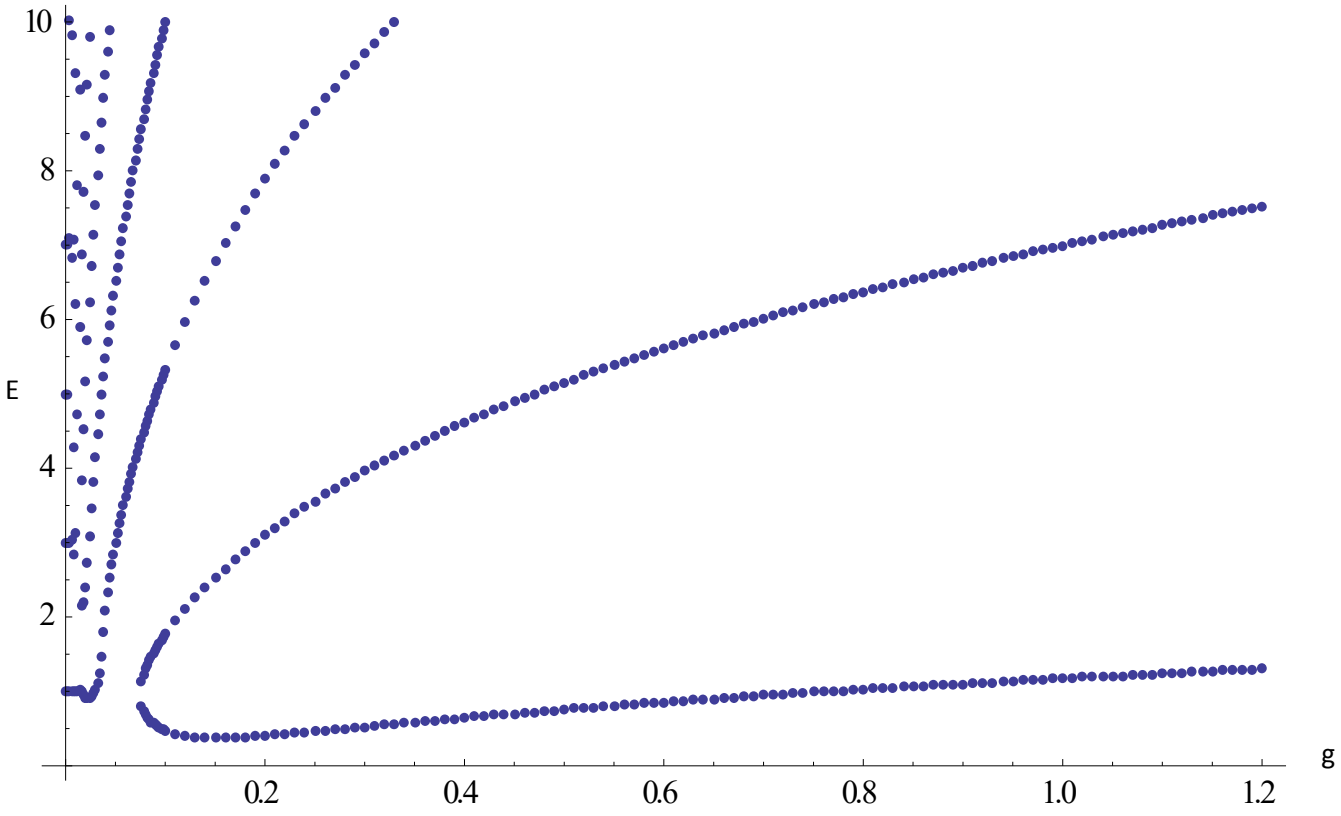


Fig 22: Eigenvalues of $x^2 - igx^5$ potential obtained using the shooting method on the complex plane up to E=10

### 5.2.3 Comparison of the eigenvalues obtained using different methods

Let us first compare the shooting on the real axis with the results from perturbation theory. We shall focus on the $0 \leq g \leq 0.2$ region, since we are interested in the region where both results agree. This time round, we calculate the perturbation series to the $400^{th}$ correction.

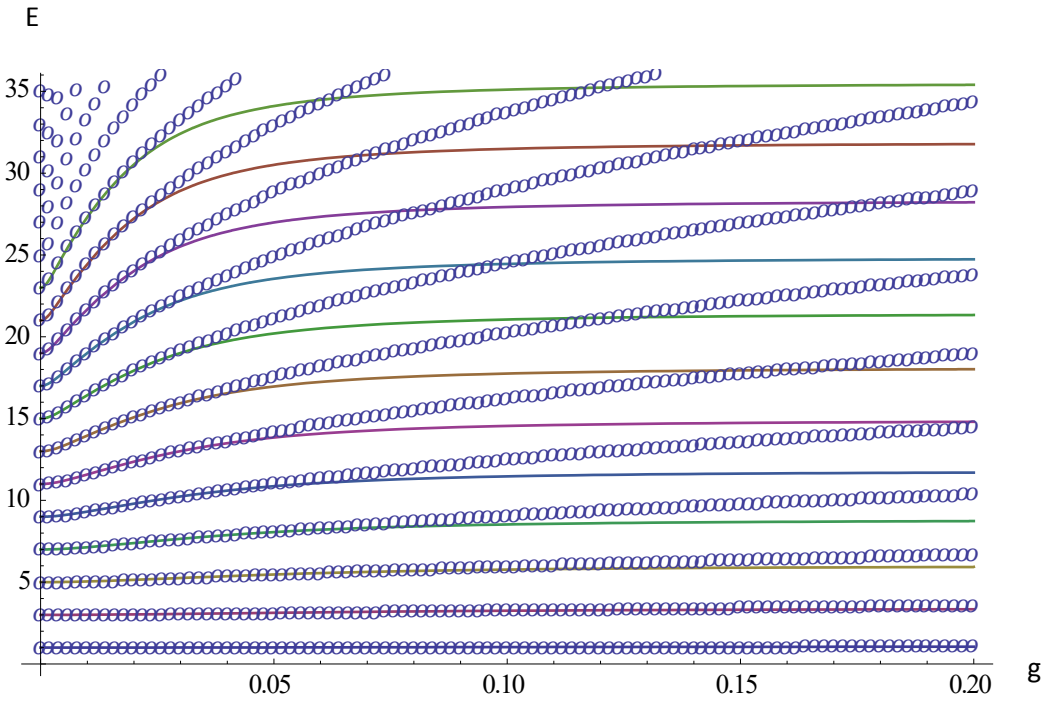


Fig 23: Eigenvalues of $x^2 - igx^5$ potential obtained using the shooting method on the real line compared with those obtained using perturbation theory. The lines are the Padé approximants while the "O" are obtained using the shooting method on the real line.

Note that the results match very closely for small values of g. We shall next compare the two graphs obtained via the shooting method with the perturbation theory results.

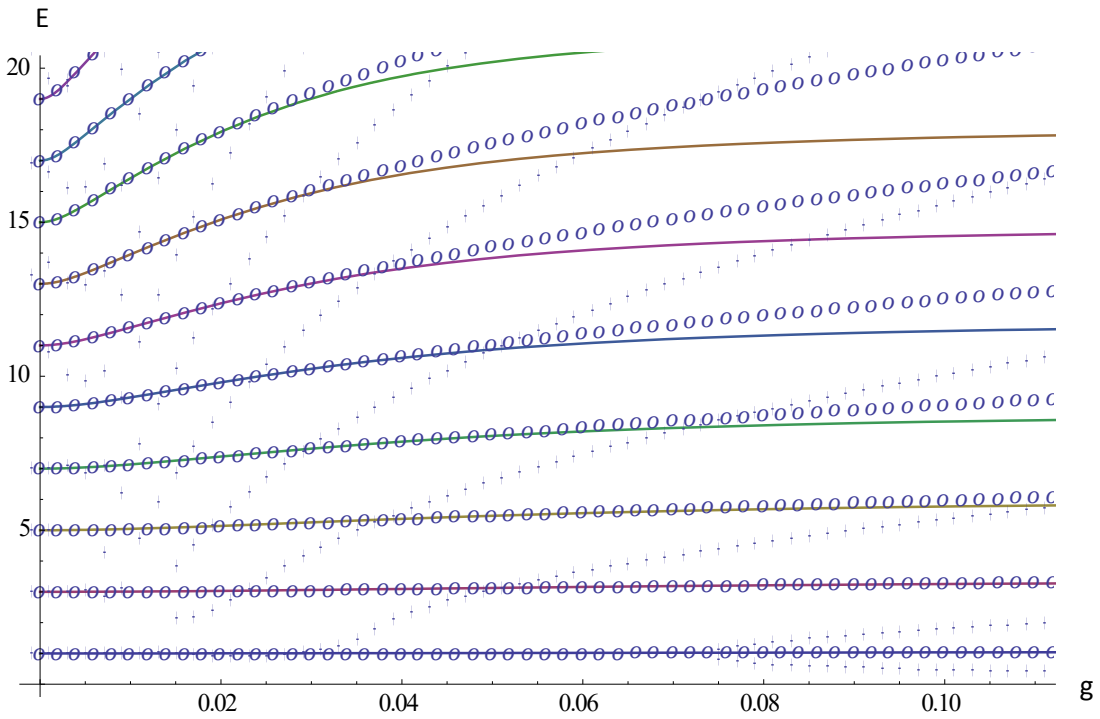


Fig 24: Comparison of Eigenvalues of $x^2 - igx^5$ potential obtained using the shooting method on the real line and on the complex plane and with Perturbation theory. The straight line is the Padé approximant, the "O" are the results obtained by shooting on the real line and the "+" are the results obtained by shooting on the complex plane.

Unlike the results obtained by shooting on the real axis, the eigenvalues obtained by shooting on the complex plane do not match the perturbation results at all. In fact, we see that the behaviour of the eigenvalues from the complex shooting is very different from the real shooting and the perturbation results. This is because by choosing to do the shooting along different paths, we have imposed different boundary conditions on the differential equation, and are hence studying different eigenvalue problems. The reason why the Padé approximation does not match the results obtained by doing the shooting on the complex plane is because the perturbed wave function contains an exponential term $e^{-\frac{x^2}{2}}$, but when we derive the wedge for which the wave function will vanish, we find that the wave function will have an real exponential term of $e^{-\frac{2}{7}\sqrt{g}r^{\frac{7}{2}}\cos(\frac{7\theta}{2}-\frac{\pi}{4})}$. Thus, the wave function obtained by shooting off the real axis and the wave function obtained using perturbation theory decay at different rates, thus perturbation theory does not agree with the results obtained from the shooting performed off the real line. The perturbation results do agree with the eigenvalues obtained by doing the shooting on the real line because when doing perturbation theory, only real numbers were involved so the analysis is essentially restricted to the real line, hence it matched up with the eigenvalues obtained by doing the shooting on the real axis.

We also do the shooting on the complex plane for small g (i.e. on a logarithmic scale). The result is shown below.

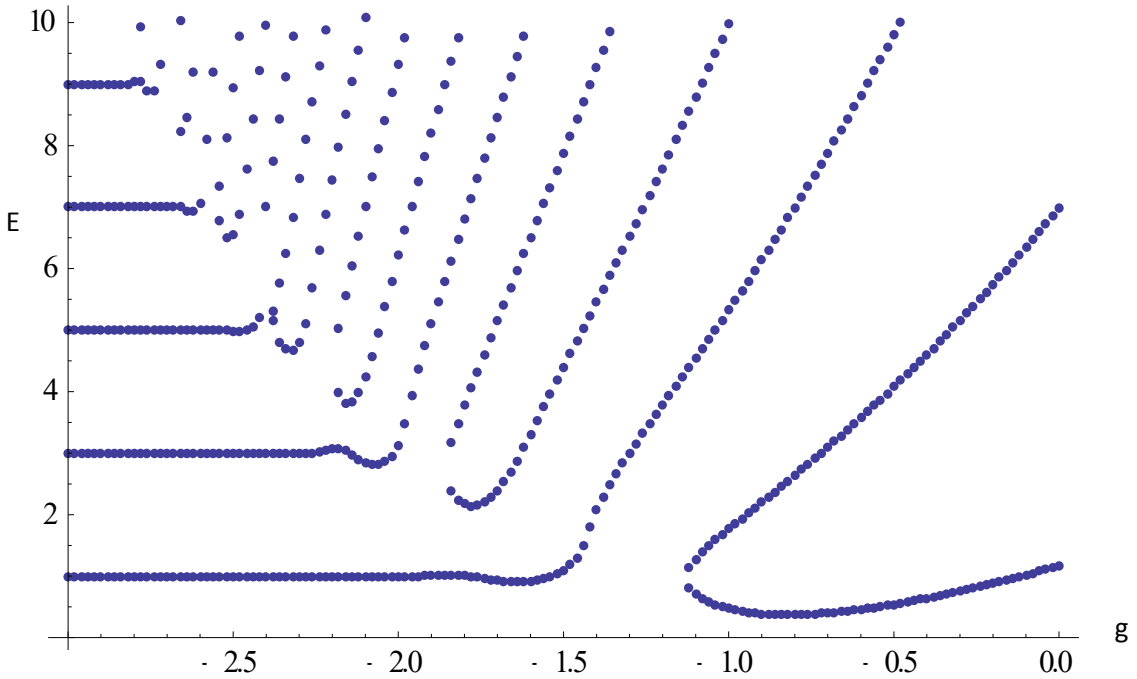


Fig 25: Eigenvalues of $x^2 - igx^5$ potential obtained using the shooting method off the real line

We note that this graph corresponds to the one that Smilga got, and we have done the shooting method for higher energy levels as well. At certain values of g, the eigenvalues cease to be real, and they become complex instead. We can see the ground state and the first excited state merging, for example. The second excited state tends to the ground state energy, which matches up with Smilga's observation. The third and fourth excited states also merge, while the fifth excited state tends to the energy level of the first excited state.

Next, we do a trick to extend our result for the shooting off the real axis further. Suppose we have a potential with a quintic perturbation.

$$\left(-\frac{d^2}{dx^2} + kx^n - igx^5\right)\psi(x) = E_g\psi(x) \tag{5.22}$$

Here, k is just a constant, and n is a positive integer. We divide by g to obtain

$$-\frac{1}{g}\frac{d^2\psi}{dx^2} + \left(\frac{k}{g}x^n - ix^5\right)\psi = \frac{E_g}{g}\psi(x) \tag{5.23}$$

Then, we make the substitution $x = ay$, where a is a constant. We then obtain

$$-\frac{1}{ga^7}\frac{d^2\psi}{dy^2} + \left(\frac{ka^{n-5}}{g}y^n - iy^5\right)\psi = \frac{E_g}{ga^5}\psi \tag{5.24}$$

Set $a = g^{-\frac{1}{7}}$. Then, we get

$$-\frac{d^2\psi}{dy^2} + \left(kg^{-\frac{n+2}{7}}y^n - iy^5\right)\psi = E_g g^{-\frac{2}{7}}\psi \tag{5.25}$$

Next, call $\lambda = g^{-\frac{n+2}{7}}$, $E_\lambda = E_g g^{-\frac{2}{7}} = E_g\lambda^{\frac{2}{n+2}}$. We end up with a Schrödinger equation where the coupling constant is attached to the other term instead.

$$-\frac{d^2\psi}{dy^2} + (k\lambda y^n - iy^5)\psi = E_\lambda\psi \tag{5.26}$$

We can then perform the shooting method on this differential equation and convert the eigenvalues by $g = \lambda^{-\frac{7}{n+2}}$, $E_g = E_\lambda\lambda^{-\frac{2}{n+2}}$. Notice that the two coupling constant g and λ are reciprocals of each other. So, when we calculate eigenvalues for small values of λ, we end up with the eigenvalues for large values of g. A more comprehensive plot of the eigenvalues is shown below.

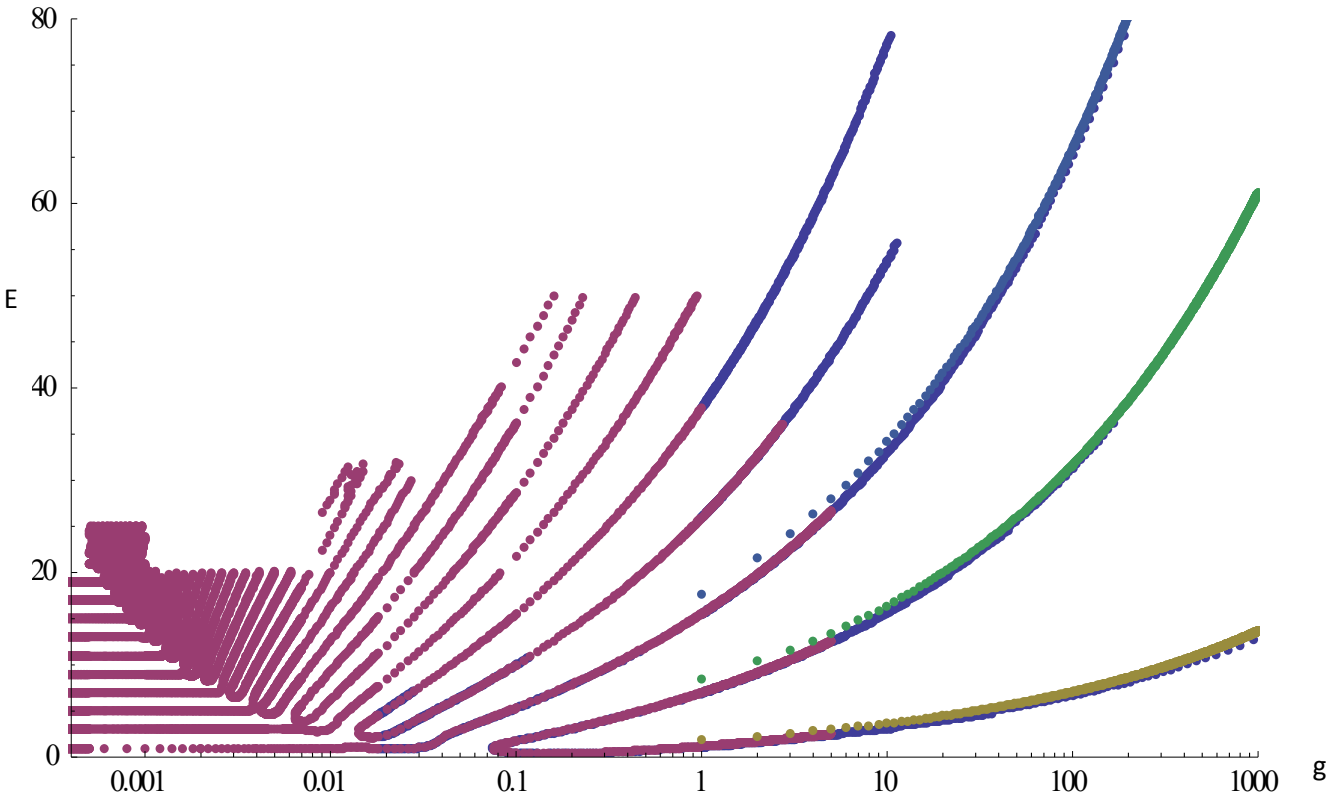


Fig 26: Eigenvalues of $x^2 - igx^5$ potential obtained using the shooting method off the real line. The coloured lines show the limit of the eigenvalues as g goes to infinity. Thus, we know that the eigenvalues remain real after $g \approx 0.074$

For this potential, we know that when $g = 0$, we recover the harmonic oscillator so the eigenvalues should be real when $g = 0$. For $g > 0.1$, we can see from the graph that the eigenvalues are real. Let us refer to the eigenstates for small values of g as the small-g eigenstates, and large-g eigenstates to refer to the eigenstates for large values of g. We also know that for large g, the potential tends to $-igx^5$ and we obtain real eigenvalues. This is the case of $\epsilon = 3$ in Bender's review paper [1].

In the graph, we have shown three lines that are the limits of the large-g ground state, 1st excited state and 2nd excited and we can clearly see that the large-g ground state, 1st excited state and 2nd excited tend to these limits as g becomes large. This tells us that the eigenvalues do become real for large values of g.

Let us take a more detailed look at the eigenvalues for smaller values of g

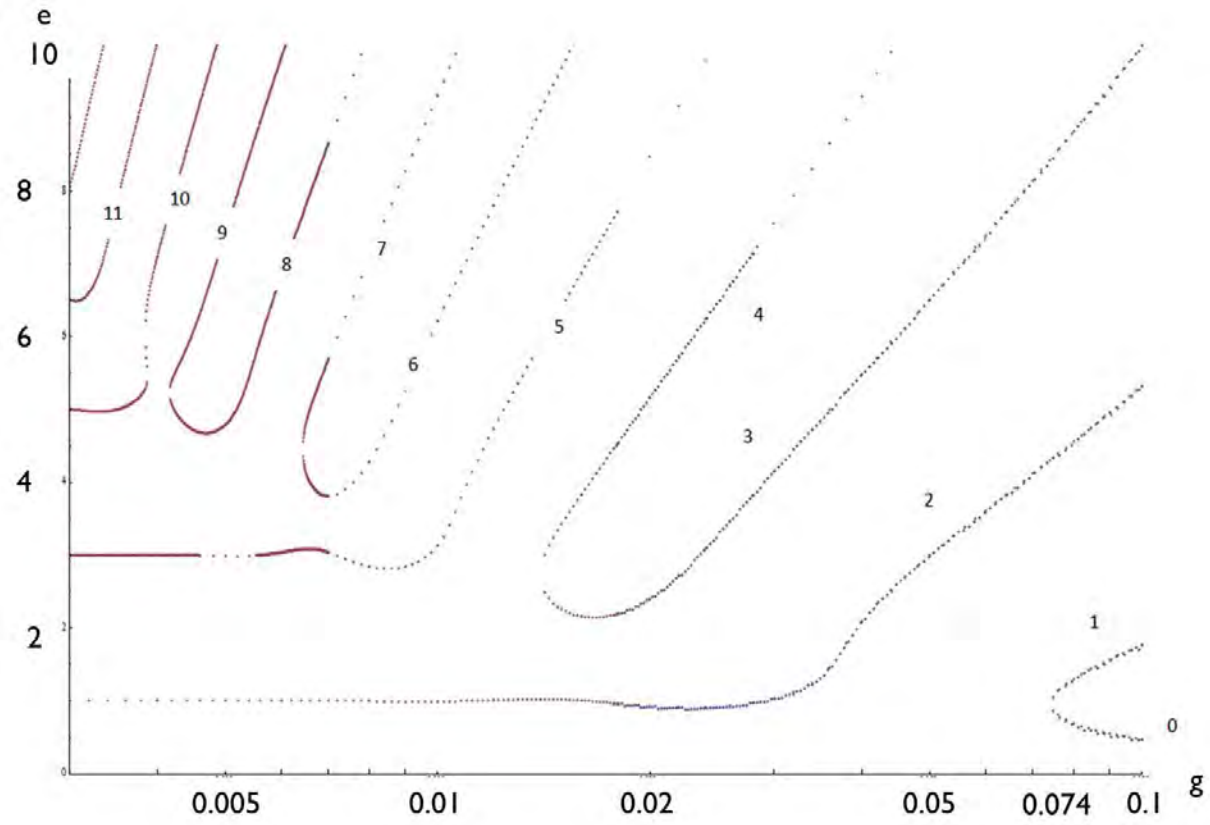


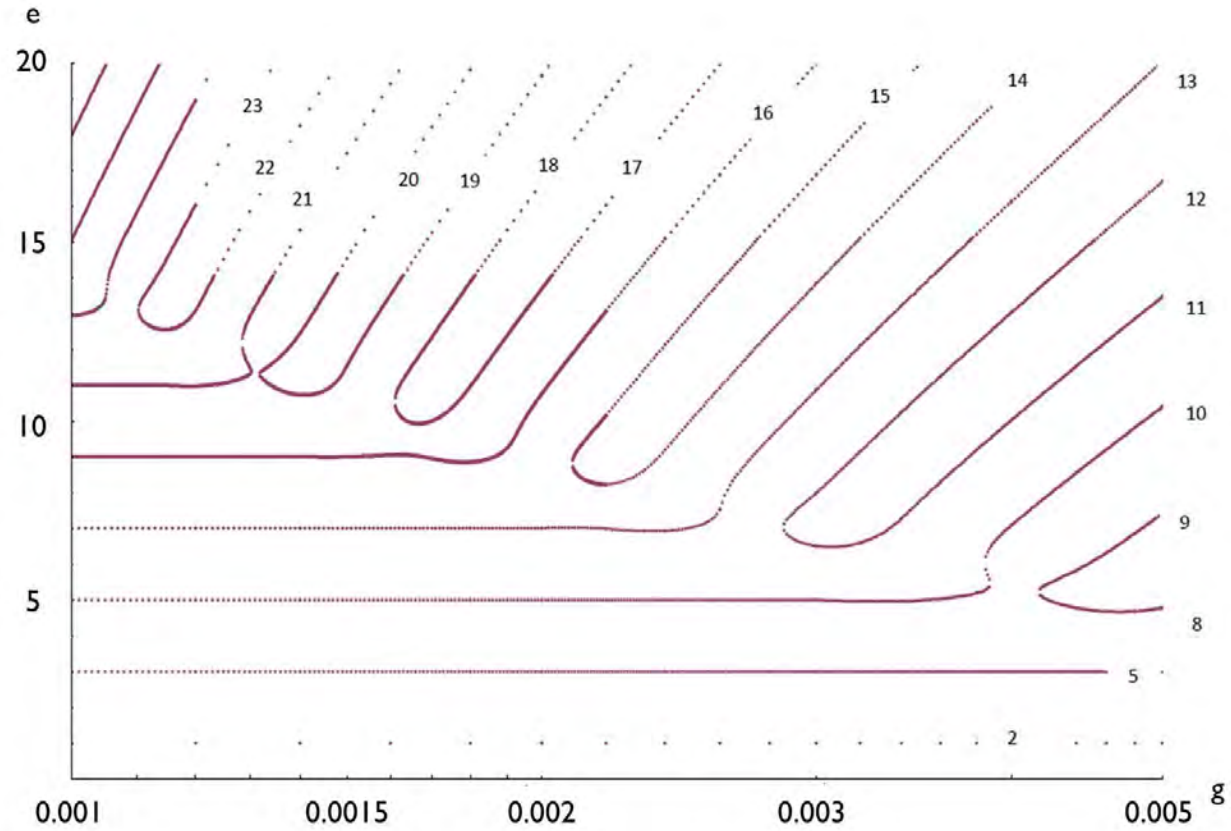

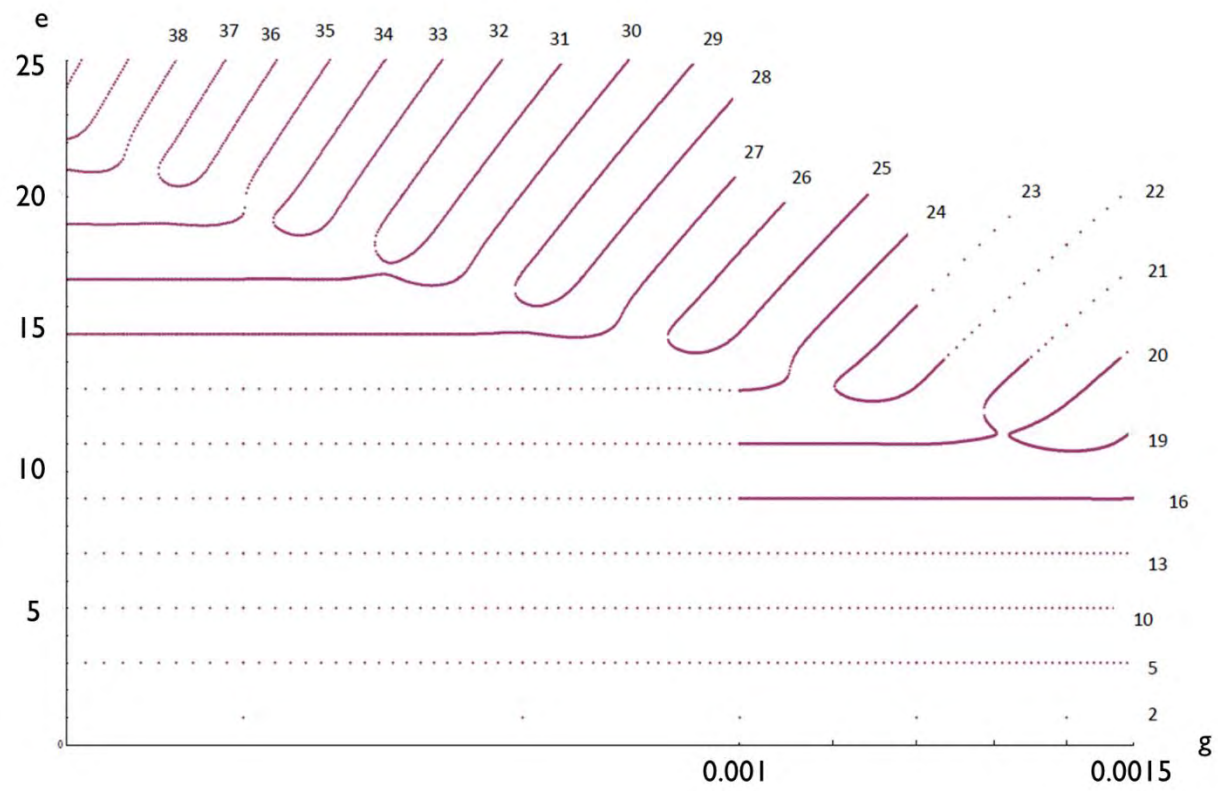


Fig 27a,b,c: Eigenvalues of $x^2 - igx^5$ potential for small values of g obtained using the shooting method off the real line

The energy levels have been labelled by the large-g eigenstates, so the "0" energy level corresponds to the ground state for the $-igx^5$ potentials. We note that for values of g smaller than $0.074$, we start to obtain complex eigenvalues. This value corresponds to the value obtained by Smilga in [7]. Looking at the graphs, the ground state and the 1st excited state merge, while the 2nd excited state remained real. The 3rd and 4th excited states merged while the 5th one remained real. The 6th and 7th, 8th and 9th states merged, while the 10th states remained real. If we look at the higher energy levels, it seems like there is a pattern of 2 states merging, followed by a state that remains real, followed by another 2 states merging, followed by a state that remains real, and then 2 consecutive pairs of energy levels merging. However, we can see that this pattern does not last by looking at the states 22, 23, 25, 26, 28 and 29.

We note, from figure 19, that the ground state and first excited state merge at about $g = 10^{-1.1}$, while the third and fourth excited states merge at about $g = 10^{-1.85}$. The values of g for which some of the higher energy levels merge and become complex keeps decreasing as the energy goes up. Here, we have two possibilities: either the values of g for

which the eigenvalues merge goes to zero as $E \to \infty$, or it tends to some $\lim_{n\to\infty} \inf g_n$. In the first case, for any small positive value of g, at high enough energies, the eigenvalues will be complex, and the Hamiltonian will have broken $\mathcal{PT}$ -symmetry since if the Hamiltonian shared eigenfunctions with $\mathcal{PT}$ then it would have real eigenvalues. In the second case, we would have a critical point $g_{crit}$ below which the Hamiltonian has unbroken $\mathcal{PT}$ -symmetry but beyond which the $\mathcal{PT}$ -symmetry is broken.

Based on our current data, it seems like there will always be complex eigenvalues for small non negative values of g. We would have a better clue if the higher energy levels can be computed. Unfortunately, doing so would require an enormous amount of computational power.

Returning to a point we made in the beginning, the value of approximately $g = 0.074$ is a point where $\mathcal{PT}$ symmetry breaking occurs. Recall that this is a phenomenon that is also observed in $\mathcal{PT}$ symmetric optics. In the last section, we shall take a look at some other Hamiltonians that are not perturbations of the simple harmonic oscillator and try to see if there is $\mathcal{PT}$ symmetry breaking.

## 6. Numerical Studies of other complex potentials

In this section, we show the eigenvalues for various complex potentials. For the potentials with the quintic term $-igx^5$, the integration path is the same, except for the $-x^4 - igx^5$ potentials, which will be explained later. For the potentials with the $-igx^3$, the integration path is the same as the ones in chapter 4 where we did the shooting method off the real line.

## 6.1 Graphs of eigenvalues versus coupling constant for various complex potentials

$$\boldsymbol{ix^3 - igx^5}$$

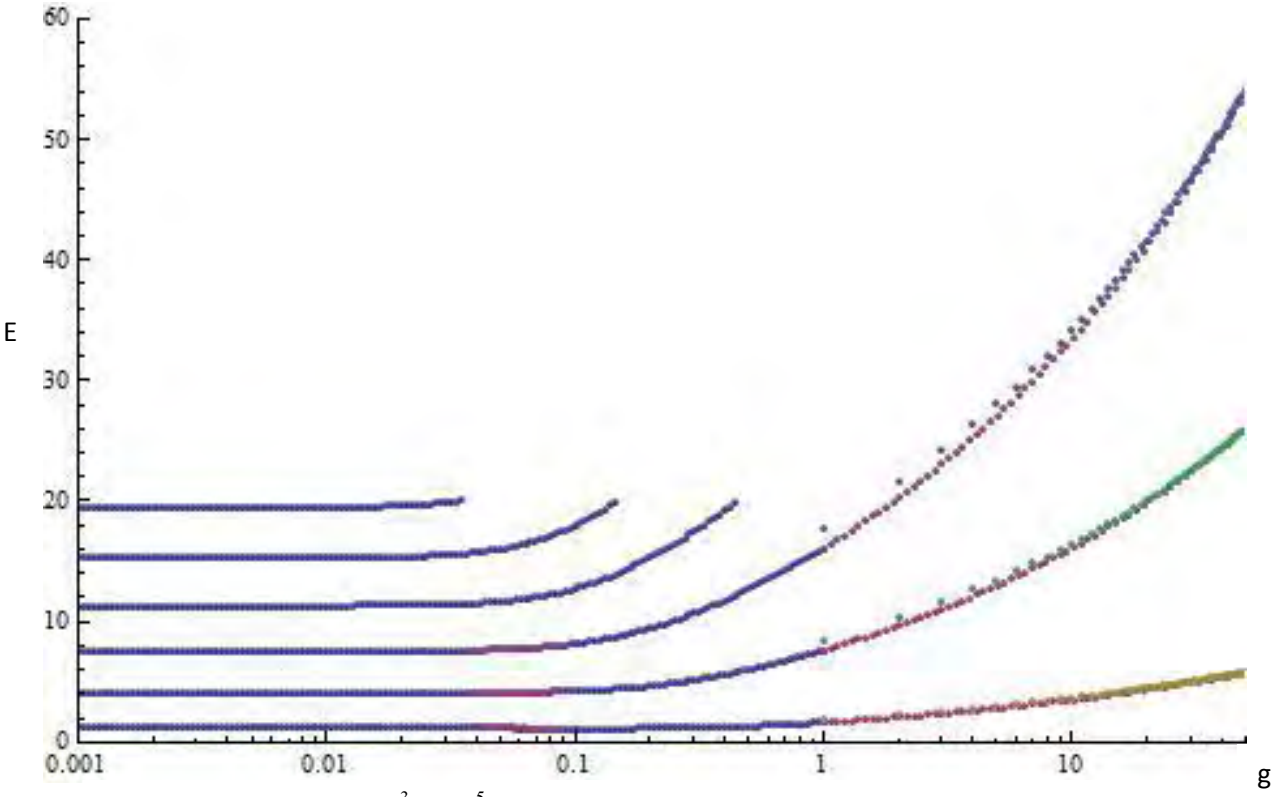


Fig 28: Eigenvalues of $ix^3 - igx^5$ potential obtained using the shooting method off the real line. The blue, green and yellow dotted lines show the correct limit of the eigenvalues for large g

The spectra is entirely real. When $g = 0$ and $g \to \infty$, we retrieve the potentials $ix^3$ and $-igx^5$, which are shown to be real in Bender's paper [3].

## $-x^4 - igx^5$

Since $-x^4$ is not much smaller than $-igx^5$ in terms of magnitude, when choosing the integration path, we had to consider the wedge for $-x^4$. We chose the integration path to be in the middle of the overlap between the wedges for $-x^4$ and $-igx^5$. The integration path is shown below.

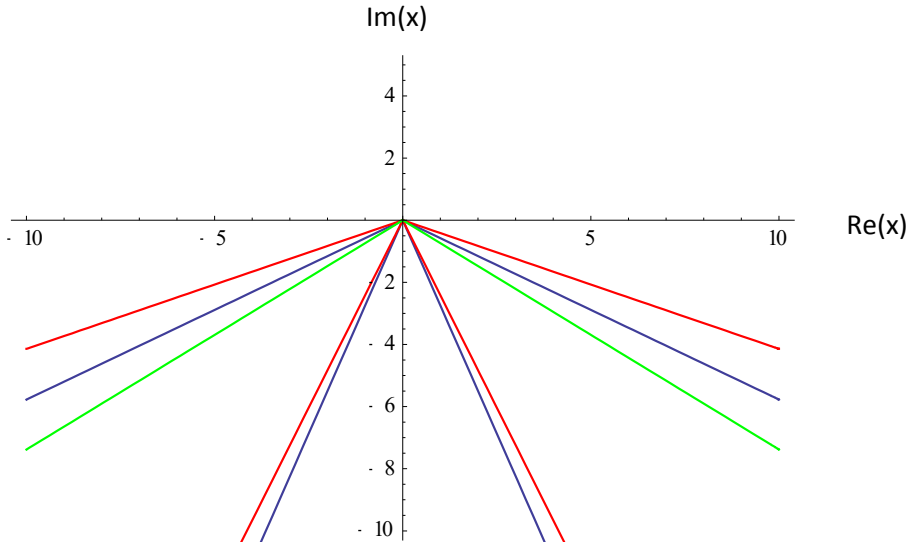


Fig 29: The red lines show the wedge for $-x^4$ while the blue lines show the wedge for $-igx^5$. The green lines are the integration paths. Notice how the $-igx^5$ wedge is closer to the imaginary axis then the $-x^4$ wedge.

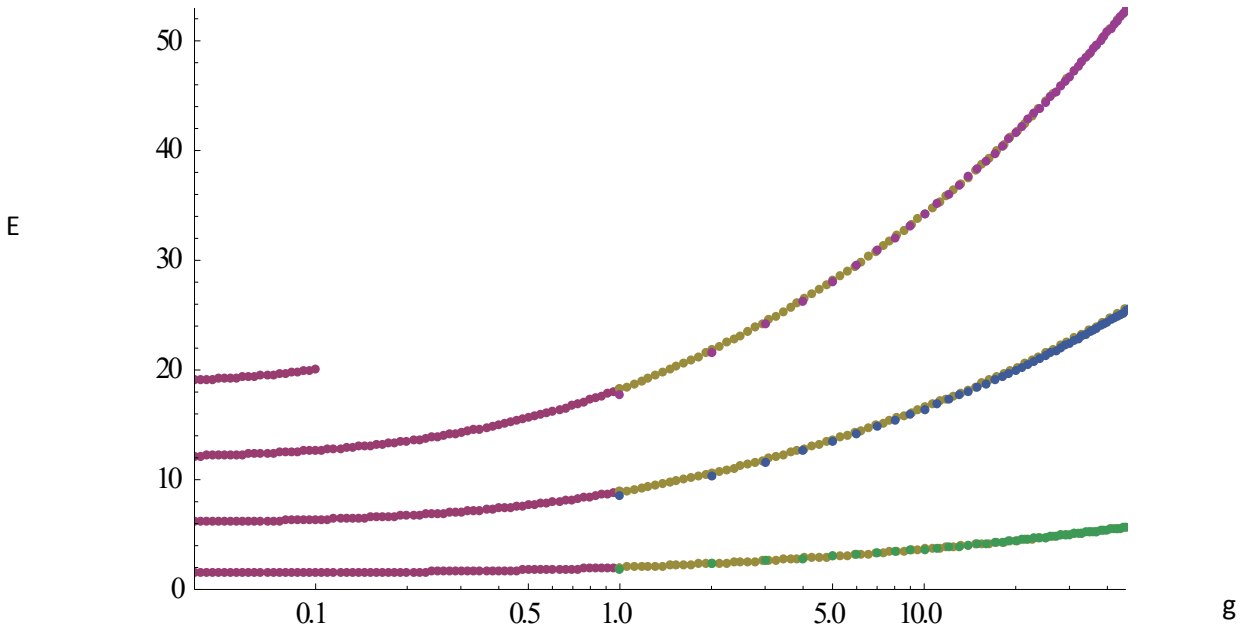


Fig 30: Eigenvalues of $-x^4 - igx^5$ potential obtained using the shooting method off the real line. The purple, blue and green lines show the correct limit of the eigenvalues for large g

When $g = 0$, we obtain the $-x^4$ which was shown to have real eigenvalues by Bender in [3]. This potential has an entirely real spectrum. The first four eigenvalues when $g = 0$ are 1.47, 6.0, 11.8, 18.45, which are in agreement with Bender's result.

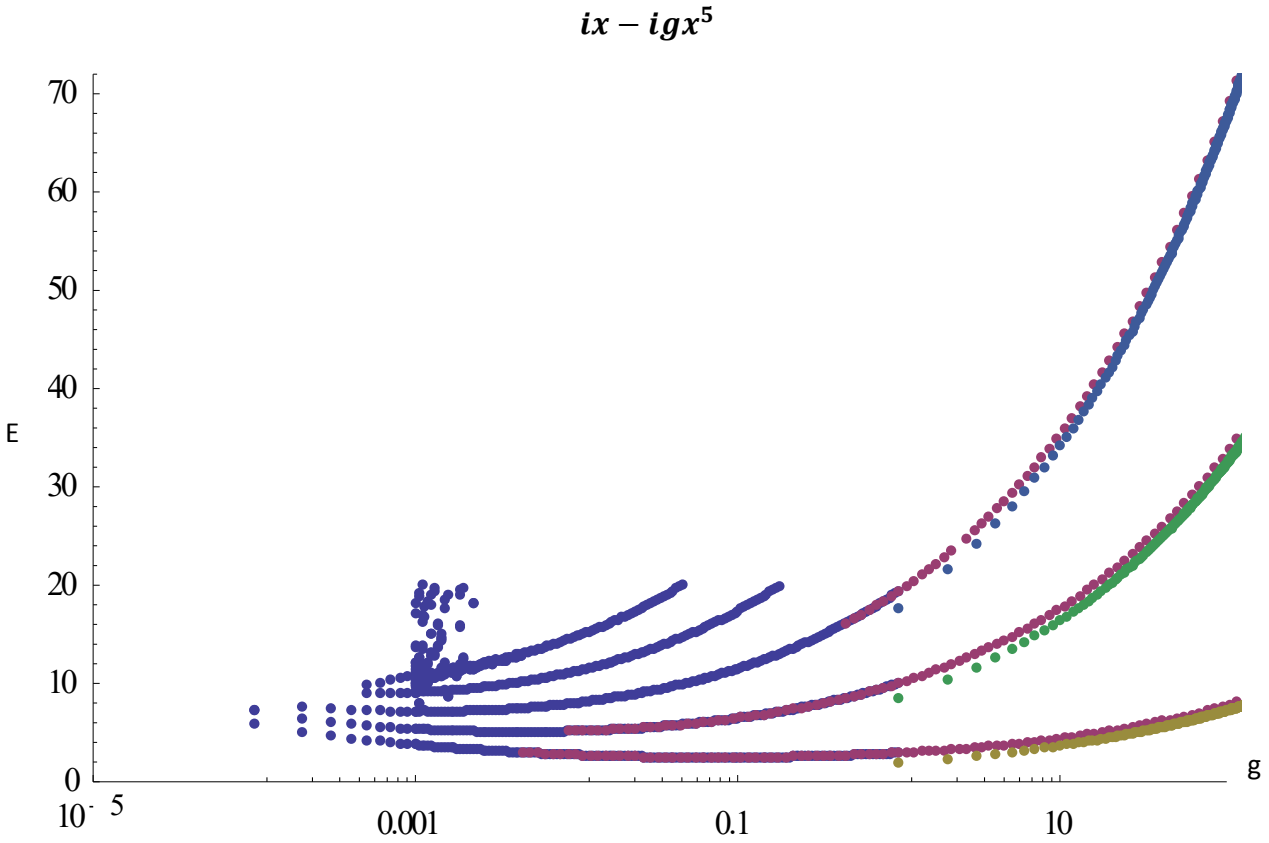


Fig 31: Eigenvalues of ix – igx$^5$ potential obtained using the shooting method off the real line. The blue, green and yellow dotted lines show the correct limits of the eigenvalues for large g.

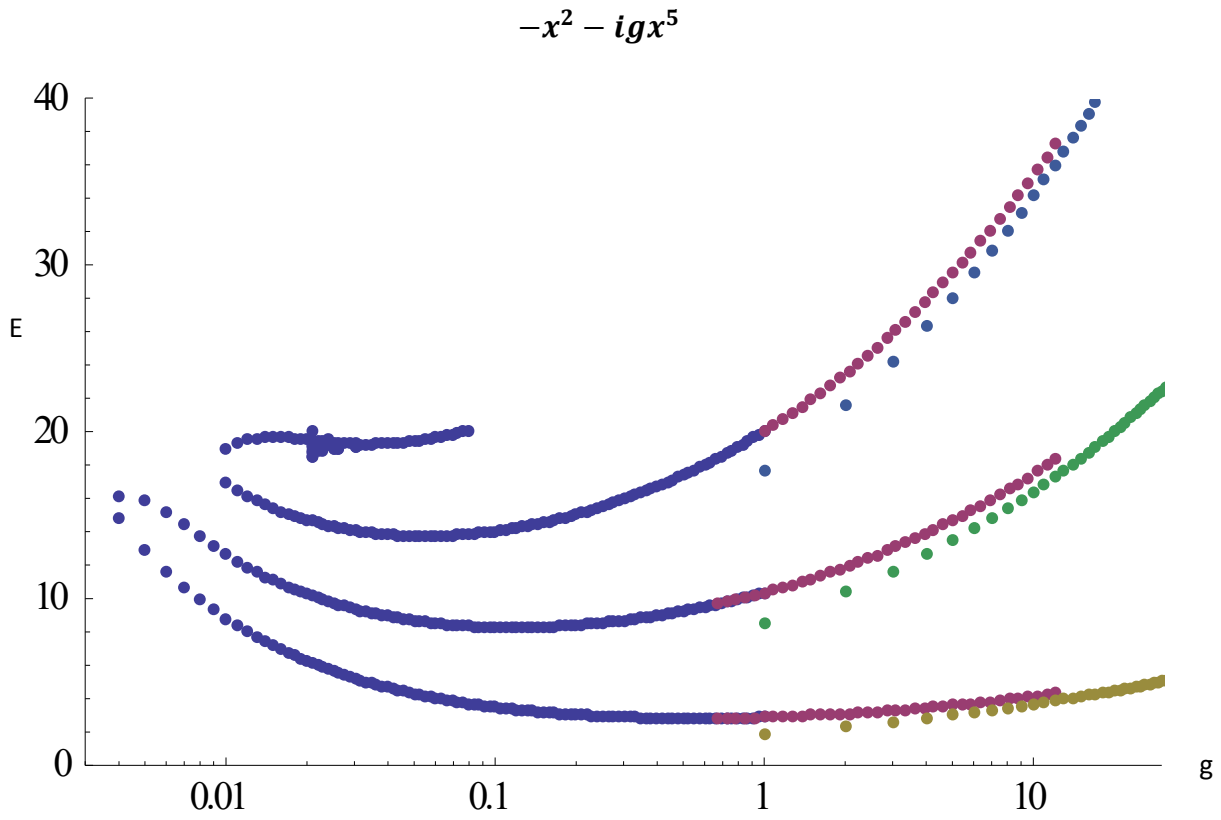


Fig 32: Eigenvalues of –x$^2$ – igx$^5$ potential obtained using the shooting method off the real line. The blue, green and yellow dotted lines lines show the correct limit of the eigenvalues for large g

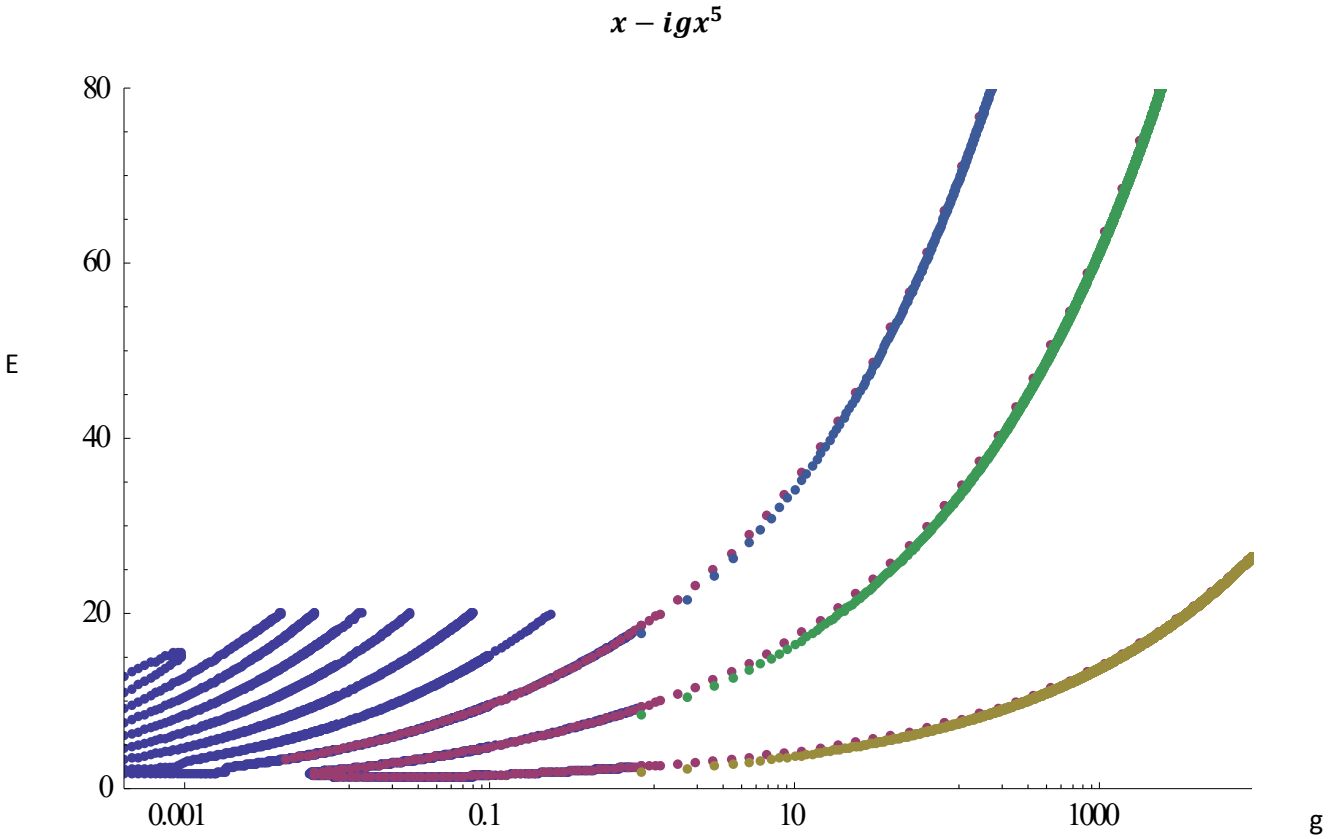


Fig 33: Eigenvalues of $x - igx^5$ potential obtained using the shooting method off the real line. The blue, green and yellow dotted lines show the correct limit of the eigenvalues for large g

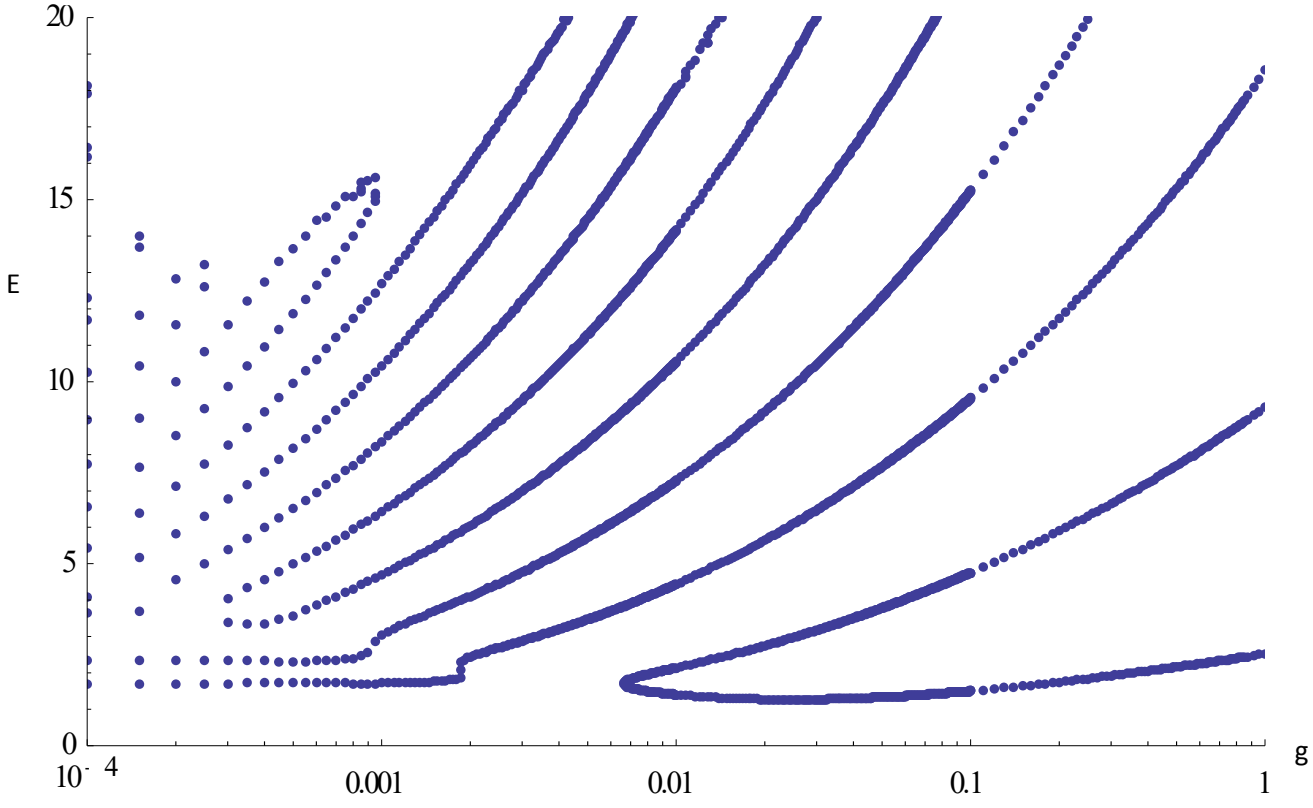


Fig 34: Eigenvalues of $x - igx^5$ potential obtained using the shooting method off the real line for small values of g

$$ix + igx^3$$

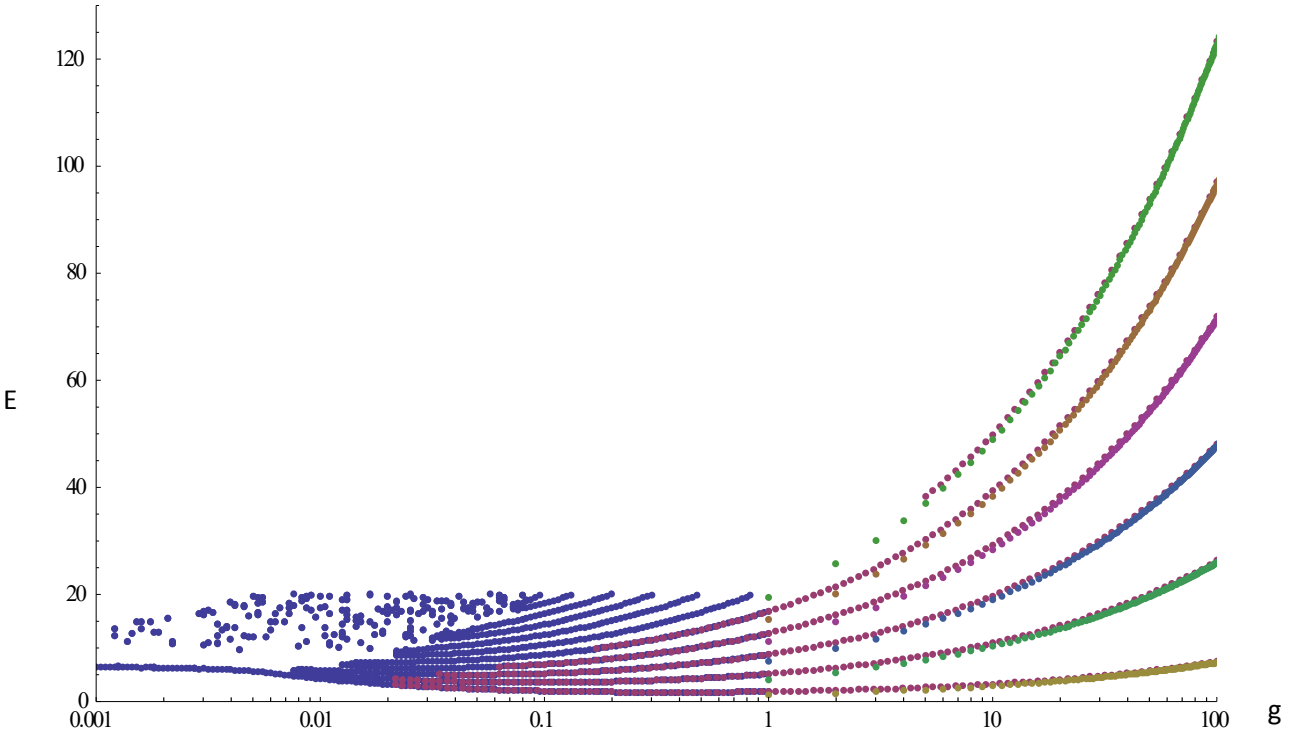


Fig 35: Eigenvalues of ix + igx$^3$ potential obtained using the shooting method off the real line. The light green, brown, purple, blue, dark green and yellow dotted lines show the correct limit of the eigenvalues for large g.

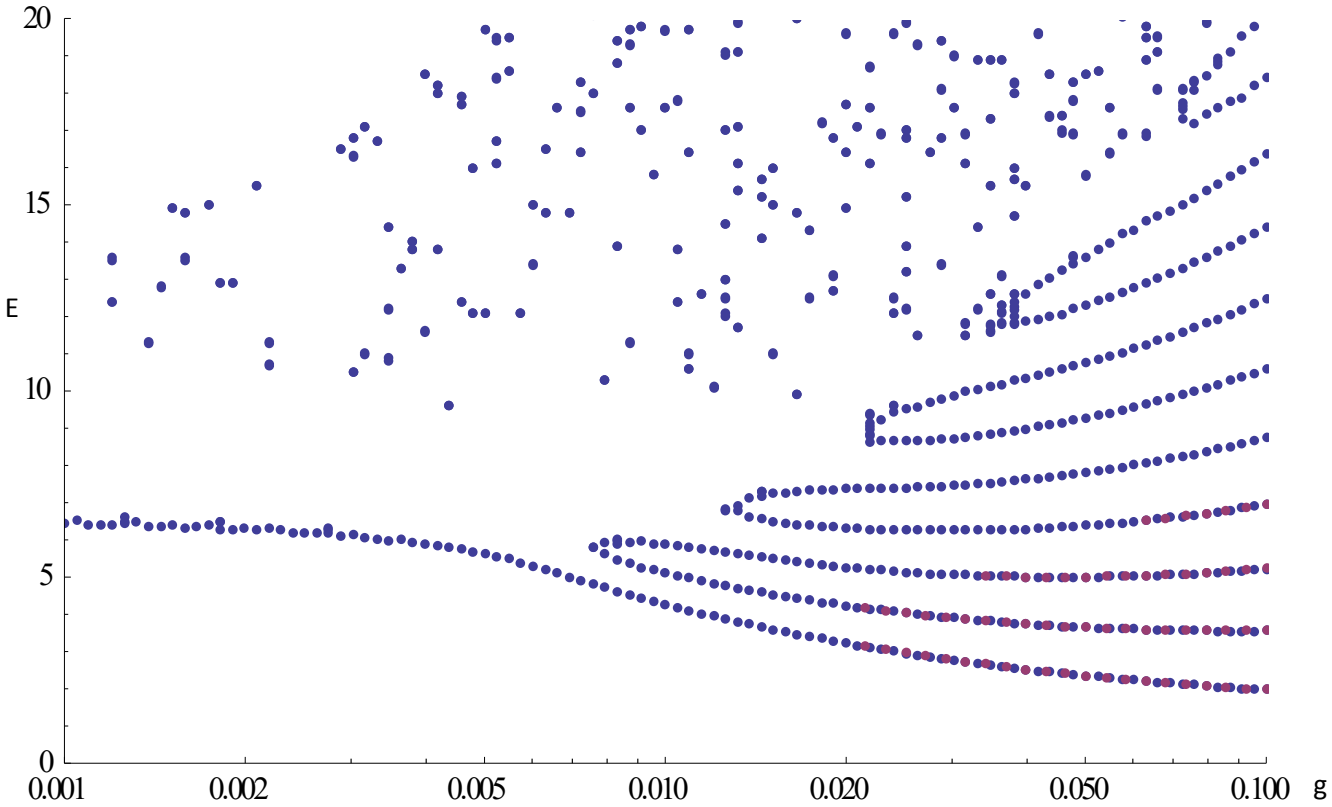


Fig 36: Closer look at eigenvalues of ix + igx$^3$ potential obtained using the shooting method off the real line for small values of g.

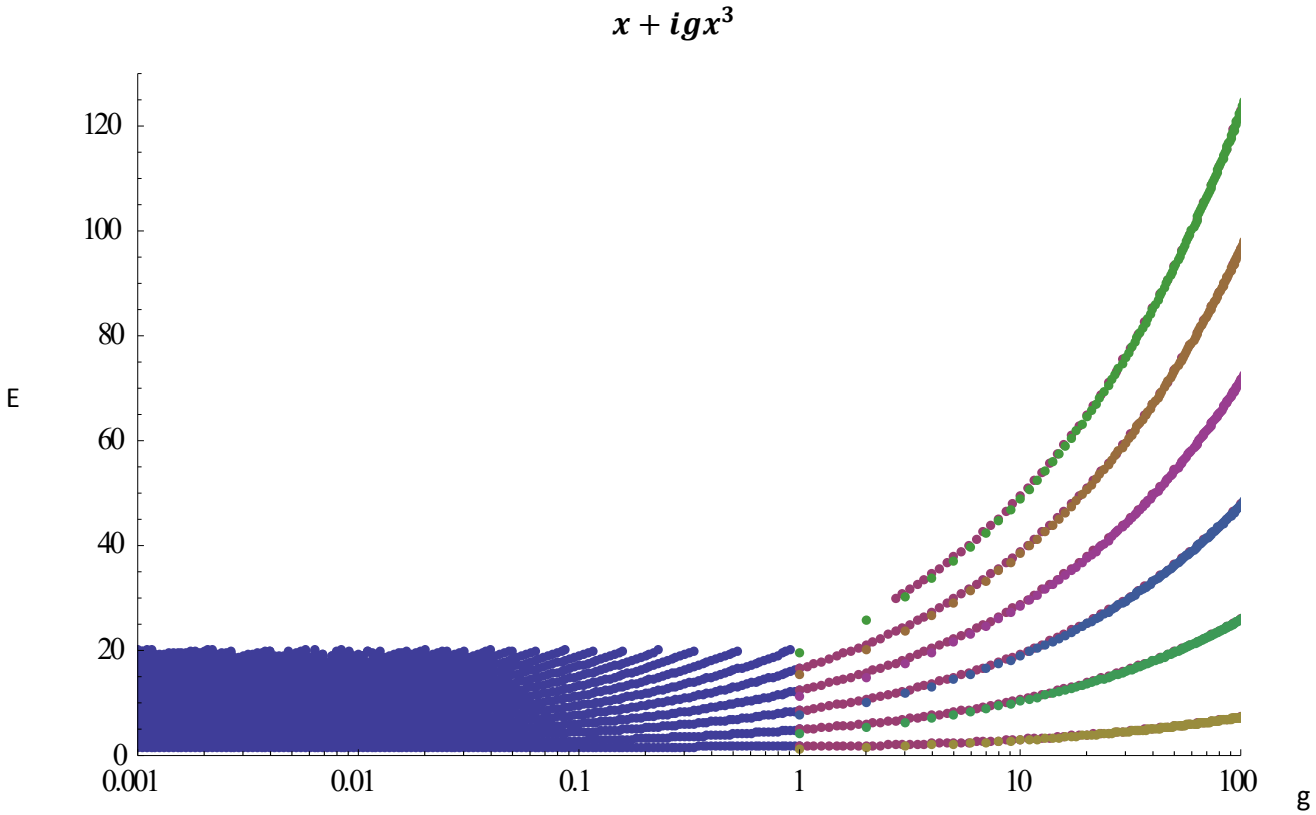


Fig 37: Eigenvalues of $x + igx^3$ potential obtained using the shooting method off the real line. The light green, brown, purple, blue, dark green and yellow dotted lines show the correct limit of the eigenvalues for large g.

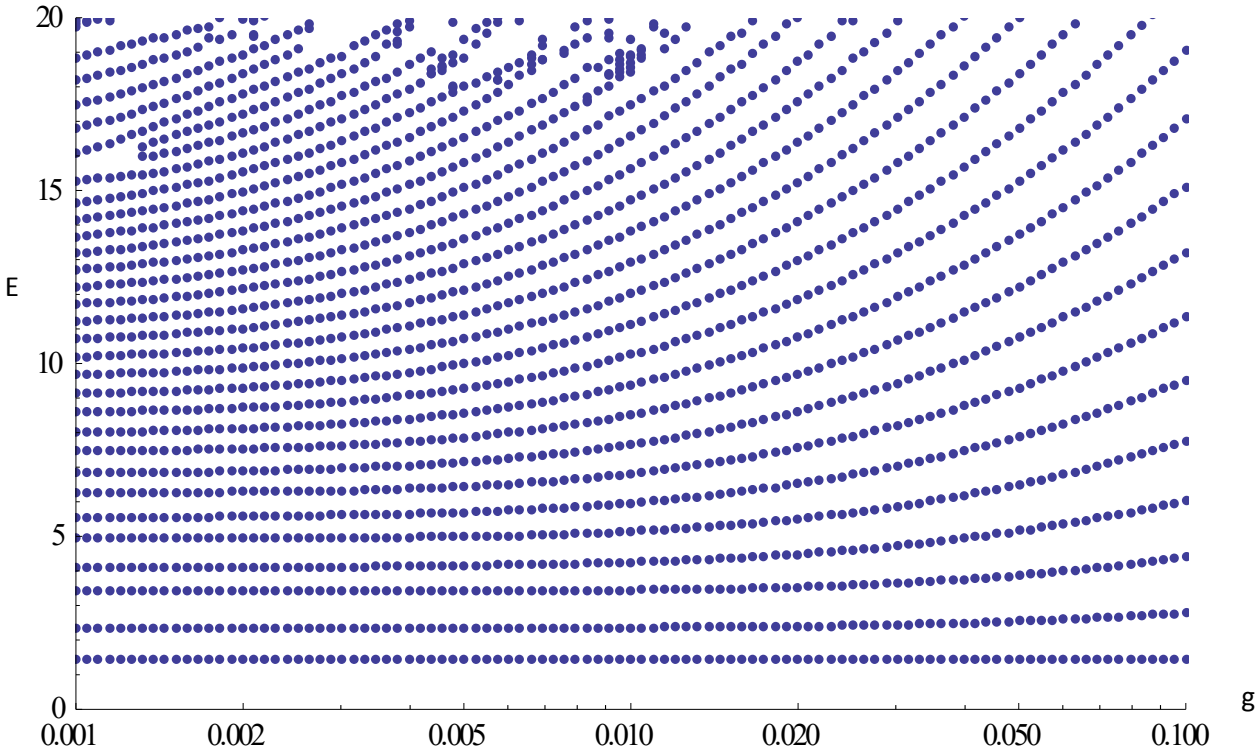


Fig 38: Closer look at eigenvalues of $x + igx^3$ potential obtained using the shooting method off the real line for small values of g.

## 6.2 Discussion

The purpose of calculating all these eigenvalues is to see if there is an explanation for $\mathcal{PT}$ symmetry breaking, and hence the appearance of complex eigenvalues. Before we discuss this further, let us make some definitions. Firstly, a Hermitian eigenvalue problem is one in which the Hamiltonian is Hermitian, and the eigenvalue problem is defined on the real line (i.e. an eigenvalue problem where the Stoke's wedges contain the real axis). A $\mathcal{PT}$ symmetric eigenvalue problem is one where the Hamiltonian commutes with $\mathcal{PT}$, and the boundary conditions are $\mathcal{PT}$ symmetric (i.e. the Stokes wedges are symmetric about the imaginary axis).

Bender conjectured that the reason for $\mathcal{PT}$ symmetry breaking for two-dimensional potentials is that there is a Hermitian term interacting with a PT symmetric one.

In our context, we see that the $x^2 - igx^5$ potential has PT symmetry breaking, and it also has a Hermitian term $x^2$ and a PT-symmetric term $-igx^5$. This agrees with Bender's conjecture, except that it is a one-dimensional system instead of a two-dimensional one.

We summarise our results in a table on the next page.

| **Potential** | **Type of terms in potential** | **Boundary Condition** | **Behaviour of eigenvalues as g goes from 0 to infinity** |
|---|---|---|---|
| $x^2+gx^4$ | Hermitian + Hermitian | Hermitian | $\mathcal{PT}$ symmetry unbroken throughout |
| $x^2+igx^3$ | Hermitian + $\mathcal{PT}$ symmetric | Hermitian | $\mathcal{PT}$ symmetry unbroken throughout |
| $x^2-igx^5$ | Hermitian + $\mathcal{PT}$ symmetric | Hermitian | $\mathcal{PT}$ symmetry unbroken throughout |
| $x^2-igx^5$ | Hermitian + $\mathcal{PT}$ symmetric | $\mathcal{PT}$ Symmetric | Inconclusive evidence for behaviour at small values of g→ $\mathcal{PT}$ symmetry broken → $\mathcal{PT}$ symmetry unbroken |
| $ix^3-igx^5$ | $\mathcal{PT}$ symmetric + $\mathcal{PT}$ symmetric | $\mathcal{PT}$ Symmetric | $\mathcal{PT}$ symmetry unbroken throughout |
| $-x^4-igx^5$ | $\mathcal{PT}$ symmetric + $\mathcal{PT}$ symmetric | $\mathcal{PT}$ Symmetric | $\mathcal{PT}$ symmetry unbroken throughout |
| $ix-igx^5$ | $\mathcal{PT}$ symmetric + $\mathcal{PT}$ symmetric | $\mathcal{PT}$ Symmetric | $\mathcal{PT}$ symmetry broken → $\mathcal{PT}$ symmetry unbroken |
| $-x^2-igx^5$ | Non-Hermitian non-$\mathcal{PT}$ + $\mathcal{PT}$ symmetric | $\mathcal{PT}$ Symmetric | $\mathcal{PT}$ symmetry broken → $\mathcal{PT}$ symmetry unbroken |
| $x-igx^5$ | Non-Hermitian non-$\mathcal{PT}$ + $\mathcal{PT}$ symmetric | $\mathcal{PT}$ Symmetric | Inconclusive evidence for behaviour at small values of g→ $\mathcal{PT}$ symmetry broken → $\mathcal{PT}$ symmetry unbroken |
| $ix+igx^3$ | $\mathcal{PT}$ symmetric + $\mathcal{PT}$ symmetric | $\mathcal{PT}$ Symmetric | $\mathcal{PT}$ symmetry broken → $\mathcal{PT}$ symmetry unbroken |
| $x+igx^3$ | Non-Hermitian non-$\mathcal{PT}$ + $\mathcal{PT}$ symmetric | $\mathcal{PT}$ Symmetric | Inconclusive evidence for behaviour at small values of g→ $\mathcal{PT}$ symmetry broken → $\mathcal{PT}$ symmetry unbroken |

Table 3: Behaviour of the eigenvalues for various complex potentials

From the table, we see that when we have a Hermitian and a $\mathcal{PT}$ symmetric term with a $\mathcal{PT}$ Symmetric boundary condition (as in the case of $x^2$-$igx^5$), we do end up with $\mathcal{PT}$ symmetry breaking, and whenever we have a $\mathcal{PT}$ symmetric potential with a $\mathcal{PT}$ symmetric boundary condition (as in the case of $ix^3$-$igx^5$ and -$x^4$-$igx^5$), we end up with real eigenvalues throughout. However, we also note that having a non-Hermitian non-$\mathcal{PT}$ symmetric term with a $\mathcal{PT}$ symmetric term and a $\mathcal{PT}$ symmetric boundary condition might also give rise to PT-symmetry breaking (e.g x-$igx^5$).

From this, it seems like having a Hermitian and a $\mathcal{PT}$ symmetric term does cause $\mathcal{PT}$ symmetry breaking, but it is not the only possible cause.

# 7. Conclusion

In this project, we have studied various complex potentials on the real axis and off it, using perturbation theory and the shooting method to solve for the eigenvalues. The results do agree with Bender's conjecture that $\mathcal{PT}$ symmetry breaking can be caused by having a Hermitian term and a $\mathcal{PT}$ symmetric term and imposing a $\mathcal{PT}$ symmetric boundary condition. As we have seen, however, that is not the only possible scenario that gives rise to $\mathcal{PT}$ symmetry breaking. This suggests the richness of the $\mathcal{PT}$ symmetry breaking phenomenon. More examples could be solved to give a better idea on the conditions that could be the cause of $\mathcal{PT}$ symmetry breaking.

Another possible direction for future work could be to study two-dimensional or higher potentials to find more examples of $\mathcal{PT}$ symmetry breaking.

# 8. References


[1] C. M. Bender and S. Boettcher, Reports on Progress in Physics. **70**, 947-1018 (2007).

[2] A. A. Andrianov, Ann. Phys **140**, 82 (1982)

[3] C. M. Bender and S. Boettcher, Phys. Rev. Lett. **80**, 5243 (1998).

[4] C.E. Rüter, K.G. Makris, R. El-Ganainy, D.N. Christodoulides, M. Segev, D. Kip, Nature Physics **6**, 192 – 195 (2010)

[5] A. Guo, G.J. Salamo, D. Duchesne, R. Morandotti, M. Volatier-Ravat, V. Aimez, G.A. Siviloglou, D.N. Christodoulides Phys. Rev. Lett. **103**, 093902 (2009)

[6] C. M. Bender and T. T. Wu, Physical Review **184**, 1231 (1969).

[7] A.V. Smilga, *J. Phys. A: Math. Theor.* **41** 244026 (2008).

[8] C. M. Bender and A. Turbiner Physics Letters **A 173**, 442 (1993)

[9] D.J. Griffiths, Introduction to Quantum Mechanics, 2nd Ed, Pearson Prentice Hall (2004).

[10] Q.H. Wang, Pramana Journal of Physics **73**, 2, 315-322 (2009)

[11] Y.N. Joglekar, C. Thompson, D.D. Scott, G. Vemuri, Eur. Phys. J. Appl. Phys. **63**: 30001 (2013).

[12] C. M. Bender and H. F. Jones, Journal of Physics A: Mathematical and Theoretical **41**, 244006 (2008)

# Appendix

In the appendix, we show some of the codes used to calculate the eigenvalues for the Hamiltonian in chapter 5. The first code is the one used to calculate the perturbation series of the ground state.

```
(*Ground State*)
n = 0; For[m = 0, m ≤ n, m++,
 B0[0, m] = Coefficient[HermiteH[n, x], x, m]]; A0[0] = 2 n + 1;
r = 1;
B0[r, n] = 0; j = 5 r + n;
B0[r, j] = (-i * B0[r - 1, j - 5])/(2 j - 2 n); B0[r, 4] = 0;
For[j = 3, j ≥ 1, j = j - 1,
 B0[r, j] = ((j + 1) (j + 2) B0[r, j + 2])/(2 j - 2 n);]; j = n;
A0[r] = (-(j + 1) (j + 2) B0[r, j + 2] + (2 j - 2 n) B0[r, j])/B0[0, j];
For[r = 2, r ≤ 200, r++,
  B0[r, n] = 0;
  For[j = 5 r + n, j ≥ 5 r + n - 1, j = j - 1,
   B0[r, j] = 1/(2 j - 2 n)
     (-i * B0[r - 1, j - 5] +
       Sum[A0[r - s] * If[j ≤ (5 s + n), B0[s, j], 0], {s, 1, r - 1}]);];

  For[j = 5 r + n - 2, j ≥ 5, j = j - 1,
   B0[r, j] = 1/(2 j - 2 n)
     ((j + 1) (j + 2) B0[r, j + 2] - i * B0[r - 1, j - 5] +
       Sum[A0[r - s] * If[j ≤ (5 s + n), B0[s, j], 0], {s, 1, r - 1}]);];
  For[j = 4, j ≥ 1, j = j - 1,
```

```
B0[r, j] = 1/(2 j - 2 n)
    ((j + 1) (j + 2) B0[r, j + 2] +
      Sum_{s=1}^{r-1} A0[r - s] * If[j ≤ (5 s + n), B0[s, j], 0]);]; j = n;
A0[r] = 1/B0[0, j]
  (-(j + 1) (j + 2) B0[r, j + 2] + (2 j - 2 n) B0[r, j] -
    Sum_{s=1}^{r-1} A0[r - s] * If[j ≤ (5 s + n), B0[s, j], 0]);
];
A0 = Table[A0[i], {i, 200}]
```

Code 01: Code used for calculating the eigenvalues of the $x^2 - igx^5$ potential obtained by perturbation theory

The following code is the code used to calculate the eigenvalues by performing shooting on the complex plane.

```
ClearAll["Global`*"];
L = 15.0; (*r value of left boundary*)
maxe = 20; (*maximum value of e we are interested in*)
mine = 0.1; (*minimum value of e we are interested in*)
ming = 0; (*minimum value of g we are interested in*)
maxg = 0.1; (*maximum value of g we are interested in*)
ince = 0.1; (*determines the increment when looking for the 1st
 decimal place of the zero. Best not to touch*)
nod = 2; (*Number of decimal places wanted*)
incg = 0.0004; (*increment in value of g*)
zeroesre = {}; (*this empty list will be used to store the zeroes
 of the matching condition function for each value of log g*)
zeroesim = {}; (*this empty list will be used to store the zeroes
 of the matching condition function for each value of log g*)
For[i = 1, i ≤ (maxg - ming)/incg + 1, i++, (*looping over the g values*)
  g = ming + incg (i - 1);
  tempstore = {}; Temporarily store the zeroes to the 1 st decimal place here
   For[j = 1, j ≤ (maxe - mine)/ince + 1, j++,
```

```
    a = mine + ince (j - 1);
    If[a == mine, θ = -3π/14;

 ratioR[r_] := -5/(4 r) + √g * e^(i (7θ/2 - π/4)) * r^(5/2); (*ψ'/ψ*)
 ratioReval = ratioR[L]; (*evaluate the WKB on the right
  wedge once and for all*)
 s = NDSolve[{e^(-2 i*θ) * y''[r] == ((r * e^(i*θ))^2 - i * g * r^5 * e^(5 i*θ) - a) * y[r],
    y[L] == 1, y'[L] == ratioReval}, y, {r, L, 0}];
 c = ({y[0], y'[0]} /. s)[[1]]; (*psi and psi prime for the right*)
 θ = -11π/14;
 ratioL[r_] := -5/(4 r) + √g * e^(i (7θ/2 - π/4)) * r^(5/2); (*ψ'/ψ*)
 ratioLeval = ratioL[L]; (*evaluate the WKB on the left wedge
  once and for all*)
 s = NDSolve[{e^(-2 i*θ) * y''[r] == ((r * e^(i*θ))^2 - i * g * r^5 * e^(5 i*θ) - a) * y[r],
    y[L] == 1, y'[L] == ratioLeval}, y, {r, L, 0}];
 d = ({y[0], y'[0]} /. s)[[1]]; (*psi and psi prime for the left*)
 fa = Re[d[[2]]/d[[1]] - e^(-i*4π/7) * c[[2]]/c[[1]]];, fa = fb];
b = a + 0.1;
θ = -3π/14;

 s = NDSolve[{e^(-2 i*θ) * y''[r] == ((r * e^(i*θ))^2 - i * g * r^5 * e^(5 i*θ) - b) * y[r],
    y[L] == 1, y'[L] == ratioReval}, y, {r, L, 0}];
 c = ({y[0], y'[0]} /. s)[[1]]; (*psi and psi prime for the right*)
 θ = -11π/14;
 s = NDSolve[{e^(-2 i*θ) * y''[r] == ((r * e^(i*θ))^2 - i * g * r^5 * e^(5 i*θ) - b) * y[r],
    y[L] == 1, y'[L] == ratioLeval}, y, {r, L, 0}];
 d = ({y[0], y'[0]} /. s)[[1]]; (*psi and psi prime for the left*)
 fb = Re[d[[2]]/d[[1]] - e^(-i*4π/7) * c[[2]]/c[[1]]];
 If[fa * fb < 0, tempstore = Append[tempstore, a]];
]
```

```
(*this portion of code is used to improve the decimal places
 of the eigenvalues for 2 d.p. and beyond*)
If[Length[tempstore] ≥ 1 && nod ≥ 2,
 For[k = 1, k ≤ Length[tempstore], k++,
   (*If takes care of the case when for some value of g,
   no zeroes were found to the first decimal place*)
   For[l = 2, l ≤ nod, l++,  (*iterating over the decimal places
      of eigenvalue*)

a = tempstore[[k]];
b = a + 10^-1; (*the next step*)
θ = -3π/14;
s = NDSolve[{e^(-2 i*θ) * y''[r] == ((r * e^(i*θ))^2 - i * g * r^5 * e^(5 i*θ) - a) * y[r],
   y[L] == 1, y'[L] == ratioReval}, y, {r, L, 0}];
c = ({y[0], y'[0]} /. s)[[1]]; (*psi and psi prime for the right*)
θ = -11π/14;
s = NDSolve[{e^(-2 i*θ) * y''[r] == ((r * e^(i*θ))^2 - i * g * r^5 * e^(5 i*θ) - a) * y[r],
   y[L] == 1, y'[L] == ratioLeval}, y, {r, L, 0}];
d = ({y[0], y'[0]} /. s)[[1]]; (*psi and psi prime for the left*)
fa = Re[d[[2]]/d[[1]] - e^(-i*4π/7) * c[[2]]/c[[1]]];
θ = -3π/14;
s = NDSolve[{e^(-2 i*θ) * y''[r] == ((r * e^(i*θ))^2 - i * g * r^5 * e^(5 i*θ) - b) * y[r],
   y[L] == 1, y'[L] == ratioReval}, y, {r, L, 0}];
c = ({y[0], y'[0]} /. s)[[1]]; (*psi and psi prime for the right*)
θ = -11π/14;
```

```
s = NDSolve[{e^(-2 i*θ) * y''[r] == ((r * e^(i*θ))^2 - i * g * r^5 * e^(5 i*θ) - b) * y[r],
   y[L] == 1, y'[L] == ratioLeval}, y, {r, L, 0}];
d = ({y[0], y'[0]} /. s)[[1]]; (*psi and psi prime for the left*)
fb = Re[d[[2]]/d[[1]] - e^(-i*4π/7) * c[[2]]/c[[1]]];
```

```
While[fa * fb > 0,
 a = a + 10^-1; b = a + 10^-1; (*recalculate a and b*)
 fa = fb;
 θ = -3π/14;
 s = NDSolve[{e^(-2 i*θ) * y''[r] == ((r * e^(i*θ))^2 - i * g * r^5 * e^(5 i*θ) - b) * y[r],
    y[L] == 1, y'[L] == ratioReval}, y, {r, L, 0}];
 c = ({y[0], y'[0]} /. s)[[1]]; (*psi and psi prime for the right*)
 θ = -11π/14;
 s = NDSolve[{e^(-2 i*θ) * y''[r] == ((r * e^(i*θ))^2 - i * g * r^5 * e^(5 i*θ) - b) * y[r],
    y[L] == 1, y'[L] == ratioLeval}, y, {r, L, 0}];
 d = ({y[0], y'[0]} /. s)[[1]]; (*psi and psi prime for the left*)
 fb = Re[d[[2]]/d[[1]] - e^(-i*4π/7) * c[[2]]/c[[1]]];

       d = ({y[0], y'[0]} /. s)[[1]];
       (*psi and psi prime for the left*)
       fb = Re[d[[2]]/d[[1]] - e^(-i*4π/7) * c[[2]]/c[[1]]];
      ];
      zeroesre = Append[zeroesre, {g, a}];
     ];
    ];
   ];
];
zeroesre
```

Code 02: Code used for calculating the eigenvalues of the $x^2 - igx^5$ potential obtained by shooting off the real line